Attributing land transport emissions to ozone and ozone precursors in Europe and Germany

Mariano Mertens[1], Astrid Kerkweg[2], Volker Grewe[1,3], Patrick Jöckel[1], and Robert Sausen[1]

[1]Deutsches Zentrum für Luft- und Raumfahrt, Institut für Physik der Atmosphäre, Oberpfaffenhofen, Germany
[2]Institut für Geowissenschaften und Meteorologie, Rheinische Friedrich-Wilhelms-Universität Bonn, Germany
[3]Delft University of Technology, Aerospace Engineering, Section Aircraft Noise and Climate Effects, Delft, the Netherlands

Correspondence: Mariano Mertens (mariano.mertens@dlr.de)

Abstract. Land transport is an important emission source of nitrogen oxides, carbon monoxide and volatile organic compounds, which serves as precursors for tropospheric ozone. Besides the direct negative impact of nitrogen oxides, air quality is also affected by these enhanced ozone tropospheric ozone concentrations. As ozone is radiativly active, its increase contributes to climate change. Due to the strong non-linearity of the ozone chemistry, the contribution of land transport emissions to tropospheric ozone cannot be calculated or measured directly, instead atmospheric-chemistry models equipped with specific source apportionment methods (called tagging) are required. In this study we investigate the contributions of land transport emissions to ozone and ozone precursors using the MECO(n) model system, coupling a global and a regional chemistry climate model, which are equipped with a tagging diagnostic. For the first time the effects of long range transport and regional effects of regional emissions are investigated. This is only possible by applying a tagging method simultaneously and consistently on the global and regional scale. We performed two three-year simulations with different anthropogenic emission inventories for Europe by applying our global model with two regional refinements, i.e. a European nest (50 km resolution) in the global model and a German nest (12 km resolution) in the European nest. We find contributions of land transport emissions to reactive nitrogen (NO_y) near ground-level in the range of 5 to 10 $nmol\,mol^{-1}$, corresponding to 50 to 70 % of the ground level NO_y values. The largest contributions are around Paris, Southern England, Moscow, the Po Valley, and Western Germany. Carbon monoxide contributions range from 30 $nmol\,mol^{-1}$ to more than 75 $nmol\,mol^{-1}$ near emission hot spots such as Paris or Moscow. The contribution of land transport emissions to ozone show a strong seasonal cycle which absolute contributions of 3 $nmol\,mol^{-1}$ during winter and 5 to 10 $nmol\,mol^{-1}$ during summer. This corresponds to relative contributions of 8 to 10 % during winter and up to 16 % during summer. Those largest values during summer are confined to the Po Valley, while the contribution in Western Europa range from 12 to 14 %. The ozone contributions are robust. Only during summer the ozone contributions are slightly influenced by the emission inventory, but these differences are smaller than the range of the seasonal cycle of the contribution. This cycle is caused by a complex interplay of seasonal cycles of other emissions (e.g. biogenic) and seasonal difference of the ozone regimes. This small difference of the ozone contributions due to the emission inventory is remarkable as the precursor concentrations (NO_x and CO) are much more affected by the change. In addition, our results suggest that during events with large ozone values the contribution of land transport emissions and biogenic emissions increase

strongly. Here, the contribution of land transport emission peak up to 28 %. Hence, land transport is an important contributor to events of large ozone values.

1 Introduction

Mobility plays a key role in everyday life, involving transport of goods and persons. Most of the transport processes rely
5   on vehicles with combustion engines, which emit not only CO_2, but also many gaseous and particulate components, such as nitrogen oxides (NO_x), volatile organic compounds (VOCs), carbon monoxide (CO) or black carbon.

The transport sector with the largest emissions is the land transport sector (involving road traffic, inland navigation and trains). Even tough the global emissions of many chemical species from the land transport sector have been decreased (e.g. Crippa et al., 2018), the emissions are still very large. For Europe and North America the emissions of NO_x from road traffic
10   have been recently discussed in the public (e.g. Ehlers et al., 2016; Ntziachristos et al., 2016; Degraeuwe et al., 2017; Peitzmeier et al., 2017; Tanaka et al., 2018). NO_x emissions influence the local air quality and lead to exceedances of the nitrogen dioxide (NO_2) thresholds in many cities. Furthermore, NO_x plays an important role for the tropospheric ozone chemistry and serves, together with CO and VOCs, as precursor for the formation of tropospheric ozone (e.g. Crutzen, 1974). Ozone is a strong oxidant and affects air quality (e.g. World Health Organization, 2003; Monks et al., 2015). Large ozone levels impact the
15   vegetation and decrease crop yield rates (e.g. Fowler et al., 2009; Mauzerall et al., 2001; Teixeira et al., 2011). Furthermore, ozone is radiatively active and thus contributes to global warming (e.g. Stevenson et al., 2006; Myhre et al., 2013).

Many studies have been performed investigating the influence of land transport emissions on ozone on the global scale (e.g. Granier and Brasseur, 2003; Niemeier et al., 2006; Matthes et al., 2007; Hoor et al., 2009; Dahlmann et al., 2011; Mertens et al., 2018), showing that land transport emissions impact ozone concentrations considerably on the global scale especially on
20   the Northern hemisphere. As has been outlined by Mertens et al. (2018) these global studies have applied different methods, rendering a comparison of the results difficult. Mostly, the so called sensitivity method (or perturbation approach) has been used, comparing results of a reference simulation with the results of a simulation in which changed emissions for the sector of interest are applied. This method calculates the impact on the concentration resulting from a change of emissions. Dahlmann et al. (2011) and Mertens et al. (2018) used a source apportionment method (by a tagged tracer approach) which calculates the
25   contribution of land transport emissions to ozone. This contribution is the part of the concentration from a specific pollutant attributed to the emissions of one specific emission source. Due to the non-linearity of the ozone chemistry the perturbation and the tagging approach give answers to different questions and therefore lead to different results (Wang et al., 2009; Emmons et al., 2012; Grewe et al., 2017; Clappier et al., 2017; Mertens et al., 2018). In teh following we use the terms 'impact' to indicate results from a sensitivity analysis and 'contribution' to refer to results of source apportionment studies. Here, we are
30   interested in the contribution of land transport emissions. Therefore, a source apportionment method is applied.

The studies discussed above investigated the effect of land transport emissions on the global scale. These results of global models, however, give only very limited information on the contribution of the land transport (or other) emissions to ozone levels on the regional scale, especially as simulated ozone concentrations depend on the model resolution (e.g. Wild and Prather,

Atmospheric
Chemistry
and Physics
Discussions

2006; Wild, 2007; Tie et al., 2010; Holmes et al., 2014; Markakis et al., 2015). Even tough, land transport is, besides other anthropogenic emissions (e.g. Matthias et al., 2010; Tagaris et al., 2014; Aulinger et al., 2016; Yan et al., 2018) and biogenic emissions (e.g. Simpson, 1995; Solmon et al., 2004; Curci et al., 2009; Sartelet et al., 2012), an important source of ozone precursors in Europe, only few studies have been performed investigating the influence of European land transport emissions

5   on ozone. Reis et al. (2000) have investigated the impact of a projected change of road traffic emissions from 1990 to 2010 on ground level ozone in Europe, reporting a general decrease of ozone levels due to emission reduction. Similarly, Tagaris et al. (2015) have applied the perturbation approach to quantify the impact of ten different emission scenarios on European ozone and PM2.5 levels using the CMAQ model for a specific period (July 2006). Tagaris et al. (2015) have quantified an impact of road transport emissions on the maximum 8-hour ozone mixing ratio of 10 % and more in Central Europe. Compared to this,

10   Valverde et al. (2016) have used a source apportionment method integrated in CMAQ (Kwok et al., 2015) to investigate the contributions of the road traffic emission of Madrid and Barcelona to ozone levels on the Iberian peninsula, reporting values of 11 to 25 %. Similarly, Karamchandani et al. (2017) have applied the source apportionment technique integrated in CAMx (Dunker et al., 2002) to calculate the contribution of eleven source categories on ozone concentrations for one summer and one winter month in 2010, focusing on 16 European cities. Generally, Karamchandani et al. (2017) have reported contributions

15   of 12 to 35 % of the road traffic sector on the ozone levels in different cities. However, in accordance with other studies Karamchandani et al. (2017) showed that European ozone levels are strongly influenced by long range transport (e.g. Jonson et al., 2018; Pay et al., 2019).

So far, all previous studies applied the source apportionment method only in a regional model. In this case the source apportionment method can attribute ozone which stem from lateral or top model boundaries not to specific emission sources.

20   Instead these contribution are quantifies as boundary contributions, which are not attributed to emission sources (Mertens et al., 2019). Accordingly, all of the previous studies have quantified only the contribution of European land transport emissions on the European ozone levels. This study is therefore dedicated to this gap of knowledge, providing a detailed assessment on the contribution of land transport emissions on ozone and ozone precursors (NO_x, CO) including European and global emissions.

To include also the effects of long range transport in regional studies, a global-regional model chain is necessary, which

25   includes a source apportionment method in the global and the regional model. Such a model is the MECO(n) model system (e.g. Kerkweg and Jöckel, 2012a, b; Hofmann et al., 2012; Mertens et al., 2016), which couples the global chemistry climate model EMAC (e.g Jöckel et al., 2010, 2016) at runtime to the regional chemistry model COSMO-CLM/MESSy (Kerkweg and Jöckel, 2012b). Both models are equipped with the MESSy interface (Jöckel et al., 2005, 2010). Due to the MESSy interface the same tagging method (Grewe et al., 2017) for source apportionment is used in the global and the regional model. Compared

30   to previous studies, this model system allows for contribution analysis from the global to the regional scale taking into account the effects of long range transport (Mertens et al., 2019). This is important as long range transport strongly influences European ozone levels.

Typically the uncertainties of such source apportionment studies are large. Typical reasons for these uncertainties are:

– uncertainties of the emissions inventories;

Atmospheric
Chemistry
and Physics
Discussions

- uncertainties in the models (e.g. chemical/physical parametrization) and differences of source apportionment methods;

- year to year variability of the contributions caused by meteorological conditions or large emissions of specific sources in specific years (for example biomass burning);

- inter annual variability of the contributions caused by meteorological conditions and seasonal cycles of emissions.

5   To account for the first three uncertainties we performed two three year long simulations with two different anthropogenic emission inventories for Europe. In our analysis we focus on mean and extreme (expressed as 95th percentile) contributions for the multi-year seasonal average values during winter (December, January, February, hereafter DJF) and summer conditions (June, July, August, hereafter JJA). We focus on results for the European domain with 50 km resolution. However, as the model resolution can influence the results, we further investigate results for a smaller domain covering only Germany with

10   12 km resolution. The manuscript is structured as follows. First, Section 2 contains a brief description of the model system, including an introduction to the applied source apportionment method as well as more details about the simulations and the applied emission inventories. Sections 3 and 4 discuss the contributions of land transport emissions to reactive nitrogen, carbon monoxide and ozone in Europe. Section 5 focuses on the contribution reactive nitrogen for Germany only based on the finer resolved simulation results. Finally, the ozone budget in Europe and the contribution of land transport emissions to the ozone

15   budget are investigated in Section 6.

2   Description of the model system

In this study the MECO(n) model system is applied (Kerkweg and Jöckel, 2012b; Hofmann et al., 2012; Mertens et al., 2016; Kerkweg et al., 2018). This system couples on-line the global chemistry-climate model EMAC (Jöckel et al., 2006, 2010) with the regional scale chemistry-climate model COSMO-CLM/MESSy (Kerkweg and Jöckel, 2012a). COSMO-CLM (COSMO

20   model in Climate Mode) is the community model of the German regional climate research community jointly further developed by the CLM-Community (Rockel et al., 2008). New boundary conditions (for dynamics, chemistry and contributions) are provided at every time step of the driving model (e.g. EMAC or COSMO-CLM/MESSy) to the finer resolved model instances (COSMO-CLM/MESSy). Accordingly, the MECO(n) model allows for a consistent zooming from the global scale into specific regions of interest.

25   The simulations analysed in the present study are the same simulations as described in detail by Mertens et al. (2019). Therefore, we present only the most important details of the model set-up. Table 1 lists the MESSy submodels applied in the present study. The global model EMAC is applied at a resolution of T42L31ECMWF, corresponding to a quadratic Gaussian grid of approx. 2.8° x 2.8° and 31 vertical hybrid pressure levels from the surface up to 10 hPa. The timestep length is set to 720 seconds. Th archive a higher resolution we apply two COSMO-CLM/MESSy nesting steps. The first refinement cov-

30   ers Europe with a horizontal resolution of 0.44° and 240 seconds time step length, while the second refinement focuses on Germany with 0.11° horizontal resolution and 120 seconds time step length. Both refinements feature 40 vertical levels from the surface up to 22 km. In the following, the abbreviation CM50 (COSMO(50 km)/MESSy) corresponds to the first refine-

ment (with roughly 50 km resolution) and CM12 (COSMO(12km)/MESSy) corresponds to the second refinement (roughly 12 km resolution). For the calculation of atmospheric chemistry the MESSy submodel MECCA is applied (Sander et al., 2011) in EMAC and COSMO-CLM/MESSy. The chemical mechanism includes the chemistry of ozone, methane and odd nitrogen. Alkynes and aromatics are not taken into account, but alkenes, and alkanes are considered up to C_4. The Mainz Isoprene Mech-

5 anism (MIM1, Pöschl et al., 2000) is applied for the chemistry of isoprene and some non-methane hydrocarbons (NMHCs). The complete namelist set-ups as well as the mechanisms of MECCA and SCAV (scavenging of traces gases by clouds and precipitation, Tost et al., 2006a, 2010) are part of the supplement.

Anthropogenic emissions as well as biomass burning, agricultural waste burning (AWB) and biogenic emissions are prescribed from external data sources (see Sect. 2.2). Emissions of soil NO_x are calculated on-line (i.e. during model runtime)

10 following the parametrisation of Yienger and Levy (1995). The same applies for emissions of biogenic VOCs which are calculated following Guenther et al. (1995), and emissions for lightning-NO_x for which the parametrisation of Price and Rind (1994) is applied.

The simulation period ranges from 07/2007 to 01/2011. The first month of 2007 are the spin-up phase and the years 2008–2010 are analysed. For reasons of computational costs CM12 has been initialised in May 2008 from CM50 and integrated for the

15 period 05/2008-08/2008 only. Therefore, results of CM12 are analysed only for JJA 2008. To facilitate a one to one comparison with observations EMAC is 'nudged' by Newtonian relaxation of temperature, divergence, vorticity and the logarithm of surface pressure (Jöckel et al., 2006) towards ERA-Interim (Dee et al., 2011) reanalysis data of the years 2007 to 2010. Sea surface temperature and sea ice coverage are prescribed as boundary conditions for the simulation set-up from this data source. The COSMO/MESSy refinements are not nudged, but forced at the lateral and top boundaries against the driving model (e.g.

20 EMAC for CM50 and CM50 for CM12).

One feature of chemistry-climate models is the coupling between chemistry, radiation and atmospheric dynamics, meaning that even small changes in the chemical state of the atmosphere lead to changes in the dynamics (which in turn feed back to the chemistry). This feedback can prevent a quantification of the influence of small emission changes on the atmospheric composition. To overcome this issue Deckert et al. (2011) proposed a so called **q**uasi **c**hemistry **t**ransport **m**odel mode (QCTM

25 mode) for EMAC, which can also be applied in MECO(n) (Mertens et al., 2016). To achieve the decoupling between dynamics and chemistry, climatologies are used within EMAC: (a) for all radiatively active substances (CO_2 , CH_4 , N_2O, CFC-11 and CFC-12) for the radiation calculations, (b) nitric acid for the stratospheric heterogeneous chemistry (in the submodel MSBM, Multiphase Stratospheric Box Model, (Jöckel et al., 2010)) and (c) for OH, O^1D and Cl for methane oxidation in the stratosphere (submodel CH4). In COSMO-CLM/MESSy only the climatology of nitric acid for the submodel MSBM is

30 required. The required climatologies are monthly mean values from the *RC1SD-base-10a* simulation described by Jöckel et al. (2016).

A set-up very similar with the set-up of this study has been evaluated with different observational data by Mertens et al. (2016). Generally, the evaluation exhibited a good agreement with observation. The biases are similar to comparable model systems and exhibit an positive ozone bias and negative biases for NO_2 and CO. One important reason for these biases is the

35 to efficient vertical mixing within the COSMO-CLM model.

2.1 Tagging method for source attribution

The source apportionment of ozone and ozone precursors is performed using the tagging method described in detail by Grewe et al. (2017), which is based on an accounting system following the relevant reaction pathways and applies the generalised tagging method introduced by Grewe (2013).

For the source apportionment the source terms, e.g. emissions, of the considered chemical species are fully decomposed in N unique categories. The definition of the ten categories considered in the current study are listed in Table 3. The tagging method is a diagnostic method, i.e. the atmospheric chemistry calculations are not influenced by the tagging method. Due to constraints with respect to the computational resources (e.g. computational time and memory) the detailed chemistry from MECCA is mapped on a family concept for which the tagging is performed. The species of the family concept are given in Table 2.

All chemical production and loss rates required for the simplified chemistry, as well as the concentration of all chemical species are obtained from the submodel MECCA. Further, loss processes like deposition are treated as bulk process, meaning that the changes of the relevant concentration due to dry- and wet deposition are memoried and later applied to all tagged species according to their contributions.

Due to the full decomposition into N categories, the sum of contributions of all categories for one species equals the total concentration of this species (i.e. the budget is closed):

$$\sum_{\text{tag}=1}^{N} O_3^{\text{tag}} \quad = \quad O_3. \tag{1}$$

To demonstrate the basic concept of the generalised tagging method we consider the production of O_3 by the reaction of NO with an organic peroxy radical (RO_2) to NO_2 and the organic oxy radical (RO):

$$NO + RO_2 \longrightarrow NO_2 + RO. \tag{R1}$$

As demonstrated by Grewe et al. (2017) (see Eq. 13 and 14 therein) the tagging method leads to the following fractional apportionment:

$$P_{R1}^{\text{tag}} \quad = \tfrac{1}{2} P_{R1} \left(\frac{NO_y^{\text{tag}}}{NO_y} + \frac{NMHC^{\text{tag}}}{NMHC} \right). \tag{2}$$

Here, all species marked with $^{\text{tag}}$ represent the quantities tagged for one specific category (e.g. land transport emissions); P_{R1} is the production rate of O_3 by reaction R1, the mixing ratios of the tagged family of NO_y and NMHC, respectively. The denominator represents the sum of the mixing ratios over all categories of the respective tagged family/species. Accordingly, the tagging scheme takes into account the specific reaction rates from the full chemistry scheme. Further, the fractional apportionment is inherent to the applied tagging method as due to the combinatorical approach, every regarded chemical reaction is decomposed into all possible combinations of reacting tagged species.

As discussed by Mertens et al. (2019) the tagging method in MECO(n) is applied in all model instances (i.e. in the global model as well as all regional model instances). Thus, consistent lateral and model top boundary conditions can be provided for the regional model instances. Compared to other source apportionment methods in regional models (e.g. Li et al., 2012; Kwok et al., 2015; Valverde et al., 2016; Pay et al., 2019) our method also attributes emissions outside the domain of the regional

5   model to specific emission sources. Source categories containing only contributions from lateral or model top boundaries are not required.

In the following, we denote absolute contributions of land transport emissions to ozone as O_3^{tra}. Analogously, contributions to the family of NO_y and CO are denoted as NO_y^{tra} and CO^{tra}, respectively (cf. abbreviations in Table 3). These absolute contribution corresponds to this shade of the species total mixing ratio which can be attributed to emissions of land transport.

10   Similarly, we investigate relative contributions given the percentage of the contribution to the total mixing ratio of the specie.

2.2   Emissions scenarios and numerical experiments

Two different emission inventories are used to investigate the uncertainties of these emission inventories. The first emission inventory is the global MACCity inventory (Granier et al., 2011), which corresponds to the RCP 8.5 emission scenario for the analysed time frame (called MAC in the following). The second emission inventory is called VEU. It is a European emission

15   inventory which has been composed in the DLR project 'Verkehrsentwicklung und Umwelt'. This emission inventory considers only the emission sectors land transport, shipping and anthropogenic non-traffic. For this emission inventory the German land transport emissions were estimated bottom up by means of macroscopic traffic simulations. Based on the travelled kilometres from the traffic simulations the land transport emissions were estimated using emission factors. For the other European countries, as well as for all other emission sectors, a top down approach has been applied. More details about the emission

20   inventory are given by Hendricks et al. (2017). Further details about the preprocessing of the emissions is given in Appendix A of Mertens (2017).

Two different simulations were performed:

-   – *REF*: The MAC emission inventory is applied in EMAC and all regional refinements (e.g. CM50 and CM12);

-   – *EVEU*: The MAC emission inventory is applied in EMAC and the VEU emission inventory in the regional refinements.

25   The VEU emission inventory contains emissions for the sectors land transport, anthropogenic non-traffic (including landing and take-off (LTO) of airplanes) and shipping. Table 4 lists the total emissions of NO_x, CO, VOC, and the ratio of NO_x to VOC for these emission sectors. In general, the total emissions of the land transport sector are quite similar, while the emissions of the anthropogenic non-traffic and shipping sectors are lower in the VEU compared to the MAC emission inventory. Especially the NO_x and VOC emissions are lower by around 30 % and 50 %, respectively. The definition of the emission sectors in VEU

30   is different from the definition in MAC. In the VEU emission inventory LTO emissions are part of the anthropogenic non-traffic sector, but inflight emissions from aircrafts are not considered in VEU. Therefore, the MAC aviation emissions are also applied in the *EVEU* simulation. To avoid a double accounting of the LTO emissions, the aviation emissions in MAC are set to zero in the lowermost level in *EVEU*, leading to a reduction of the aviation emissions of the MAC emission inventory by $0.05 \, \mathrm{Tg \, a^{-1}}$

Atmospheric
Chemistry
and Physics
Discussions

(see Table 4). For the emission sectors agricultural waste burning (AWB), biomass burning, lightning and biogenic we apply the same emissions in both simulations (see Table. 5). Total emissions for the global model EMAC, as well as for CM12 are given in the Supplement (see Section S2).

Figure 1 displays the geographical distribution of the land transport emissions of NO_x, CO, and VOC applied in the *REF*
5   and *EVEU* simulations and the difference of the emissions between both simulations. Shown are only the emissions of EMAC and CM50, focusing on Europe. The NO_x land transport emissions for CM12 are depicted in the Supplement (Fig. S7). Further, more detailed figures showing the geographical distribution in CM50 are part of the Supplement (Fig. S8). The emissions of CM50 are superimposed onto the emissions applied in EMAC, where the MACCity emissions are applied globally. For the emissions in Europe we not that despite the comparable total emissions the geographical distribution differs. Generally, the
10 VEU emission inventory features larger emissions near the hot-spots and lower emissions away from the hot-spots compared to MAC. Further, MAC features larger NO_x emissions especially the Northern part of the British Islands and in Finland. Emissions of CO are especially larger around Estonia in MAC compared to VEU. Especially over Germany, the Po Valley and party of Eastern Europe VEU features more emissions of NO_x, CO and VOC (see also totals for CM12 in Table S4). Besides the difference between the emissions applied in CM50 (and CM12) it is important to note, that for the *REF* and the *EVEU*
15 simulation the same emissions are applied in EMAC. Therefore, the difference (Fig. 1c) is zero in EMAC.
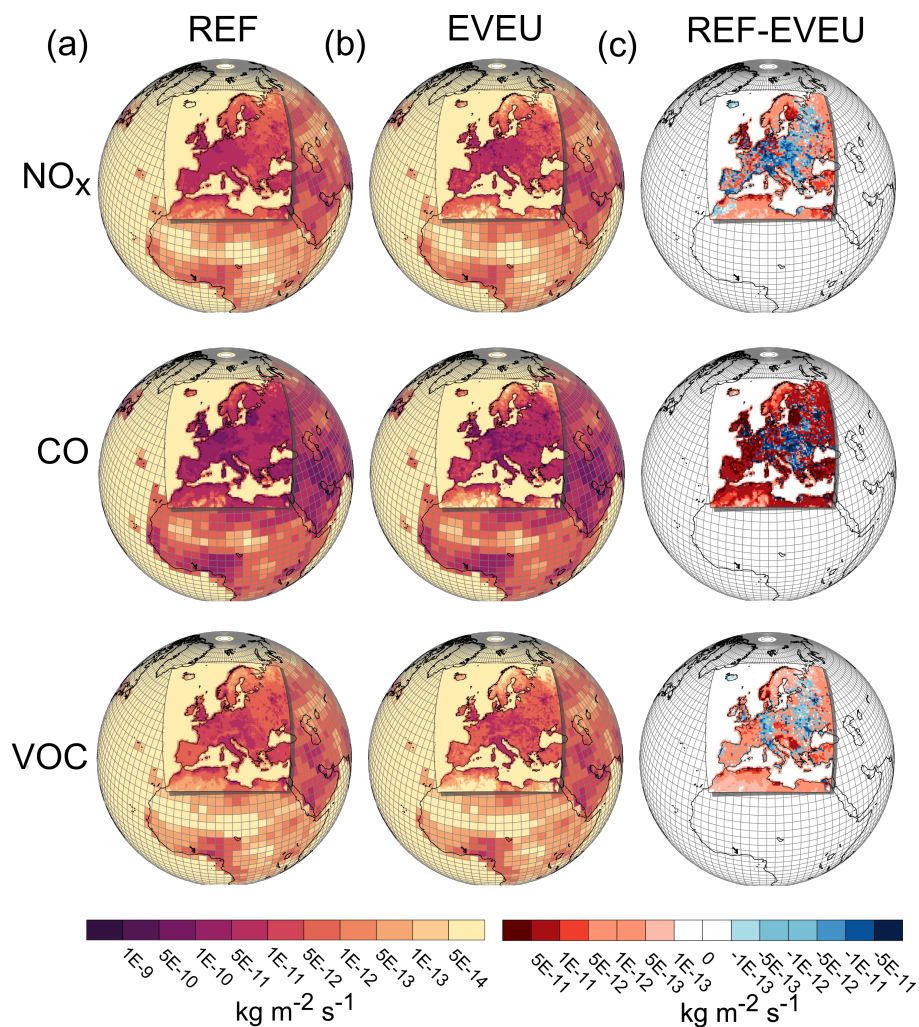
Figure 1. Annually averaged emission fluxes (2008 to 2010) from the land transport sector (in $kg\,m^{-2}\,s^{-1}$). Shown are the emissions as applied in EMAC (based on the MACCity inventory) and in CM50. The emissions of CM50 are superimposed on the emissions of EMAC. In the region covered by CM50 EMAC also uses the MACCity emissions (not visible). (a) the emissions of the *REF* simulation, (b) the emissions of the *EVEU* simulation and (c) the difference of the emissions from *REF* and *EVEU* ('REF MINUS EVEU'). Shown are the emission fluxes of of NO_x (in kg NO m^{-2} s−1), CO (in kg CO m^{-2} s−1); and VOC (in kg C m^{-2} s−1).

3 Contributions of land transport emissions to ground level mixing ratios of NO_y and CO Europe

CO and NO_y are direct pollutants of the land transport sector, with different chemical lifetimes. Please note, that the contributions to NO_y and not to NO_x are investigated as the source apportionment method tags the whole family of NO_y (without PAN) and not NO_x alone. Our focus in this section are on the results on the European scale, results of NO_y for Germany will

5 be discussed in Sect. 5. Figure 2 shows NO_y^{tra} for DJF and JJA, respectively. The largest mixing rations of NO_y^{tra} are simulated near Southern England, the Paris metropolitan region, Western Germany and the Benelux states as well as the Po Valley and the Moscow metropolitan region. In these regions contributions of up to 10 nmol mol^{-1} are simulated. In general, larger absolute contributions occur during DJF compared to JJA, but the annual cycle of the land transport emissions is small in both emission inventories (see supplement Figure S4). Accordingly, the differences of NO_y^{tra} between DJF and JJA are likely not caused by

10 seasonal differences of the emissions, but by larger mixing layer heights as well as a more effective photochemistry during JJA compared to DJF.

The seasonal change of the NO_y^{tra} is smaller than differences between *REF* and *EVEU*. Near areas with large land transport emissions *EVEU* simulates 3 to 4 nmol mol^{-1} larger contributions than *REF*. In most of the hot-spot regions (e.g. Paris and the Po Valley) the differences are even larger and the contributions calculated by *EVEU* are 5 nmol mol^{-1} larger as in *REF*.

15 In some regions the results of both simulations are in total contrast. In *REF* for example, contributions of up to 4 nmol mol^{-1} are simulated in Finland, while mixing ratios of NO_y^{tra} below 1 nmol mol^{-1} are simulated in *EVEU*.

The absolute contributions correspond to relative contributions of land transport emissions to ground level NO_y of 40 % to 70 % in most parts of Europe (see Fig 3). During DJF, *REF* simulates the lowest relative contributions of 30 to 50 % over most parts of Europe. During summer the contributions increase up to 60 % with the largest values in Southern Germany, the Po

20 Valley, and southern England. *EVEU* simulates a smaller difference of the contributions between DJF and JJA as *REF*. Further, the maxima are generally slightly larger and contributions of up to 70 % are simulated around the Po Valley and the Paris area. Interestingly, the relative contributions are lower during DJF than during JJA while the absolute contributions are larger during DJF than during JJA. Most likely this is caused by the lower amount of anthropogenic non-traffic NO_x emissions during JJA compared to DJF (see Fig. S4 in the Supplement).

25 The simulated mixing ratios of CO^{tra} (see Fig. 4) show a similar behaviour as NO_y^{tra}, implying that contributions during DJF are larger as during JJA. This seasonal difference is most likely caused by lower mixing layer heights and increased lifetime of CO during DJF compared to JJA, as OH concentrations are lower in winter compared to summer. Generally, the largest contributions are simulated in southern England, around Paris, Western Germany, the Po Valley and around Moscow. In *EVEU* contributions of up to 75 nmol mol^{-1} are simulated around London, Paris, Milan and Moscow, while the results of

30 the *REF* simulation show lower contributions in the Western European regions of mostly 50 to 60 nmol mol^{-1}. Compared to NO_y^{tra}, however, some hot-spots stand out in the results of the two simulations. *EVEU*, for example, shows larger contributions (40 to 60 nmol mol^{-1}) to CO over Hungary or southern Poland. In difference to this, *REF* shows contributions of 30 to 50 nmol mol^{-1} over Estonia. These differences of the contributions are directly caused by differences between the two
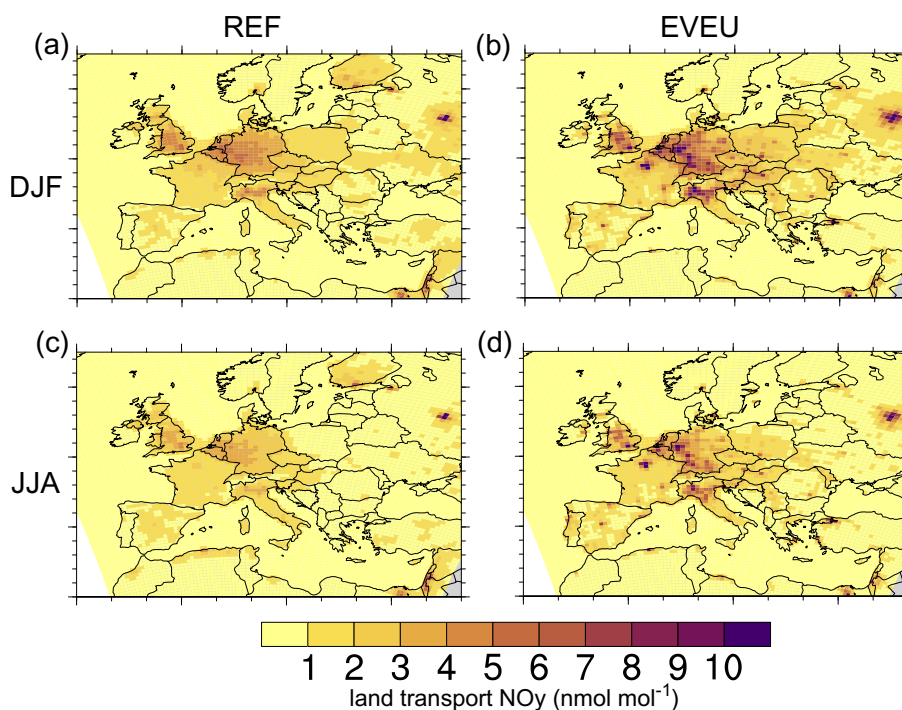
Figure 2. Absolute contribution of land transport emissions to ground-level NO_y (in $\mathrm{nmol\,mol^{-1}}$) as simulated by CM50. (a) and (b) contributions for the period DJF (2008 to 2010) of the *REF* and *EVEU* simulations, respectively. (c) and (d) contributions for the period JJA (2008 to 2010) of the *REF* and *EVEU* simulations, respectively.

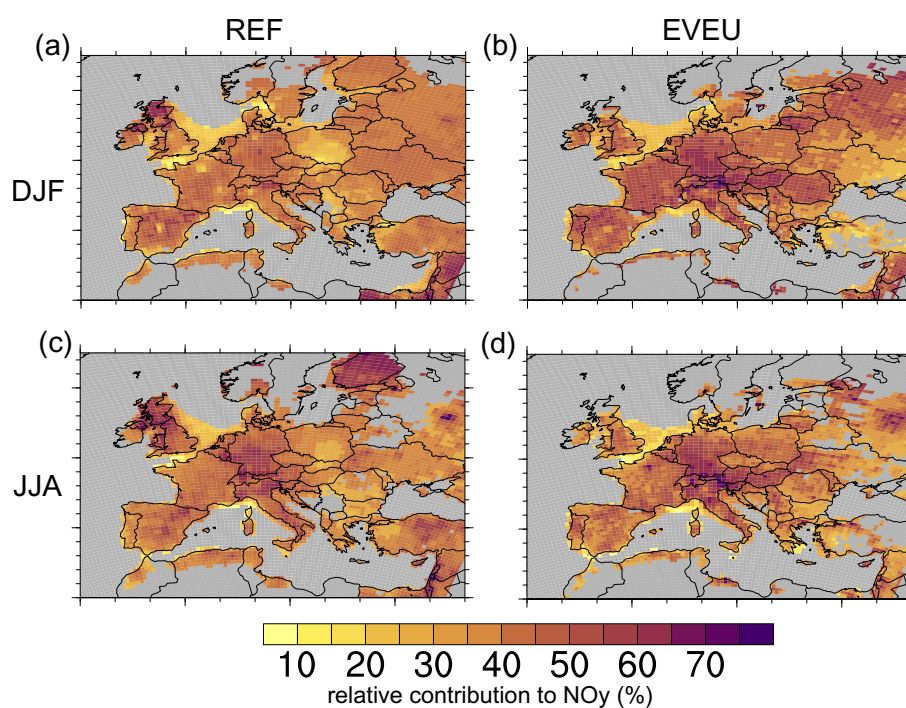emission inventories (Fig. 1). Hence, the uncertainties with respect to the CO emissions of land transport in these regions are quite large.

Figure 3. Relative contribution of land transport emissions to ground-level NO_y (in %) as simulated by CM50. (a) and (b) contributions for the period DJF of the *REF* and *EVEU* simulations, respectively. (c) and (d) contributions for the period JJA of the *REF* and *EVEU* simulations, respectively. Grey areas indicate regions where the absolute NO_y mixing ratios are below $0.5 \ \mathrm{nmol \ mol^{-1}}$. In these regions no relative contributions are calculated for numerical reasons.

Atmospheric
Chemistry
and Physics
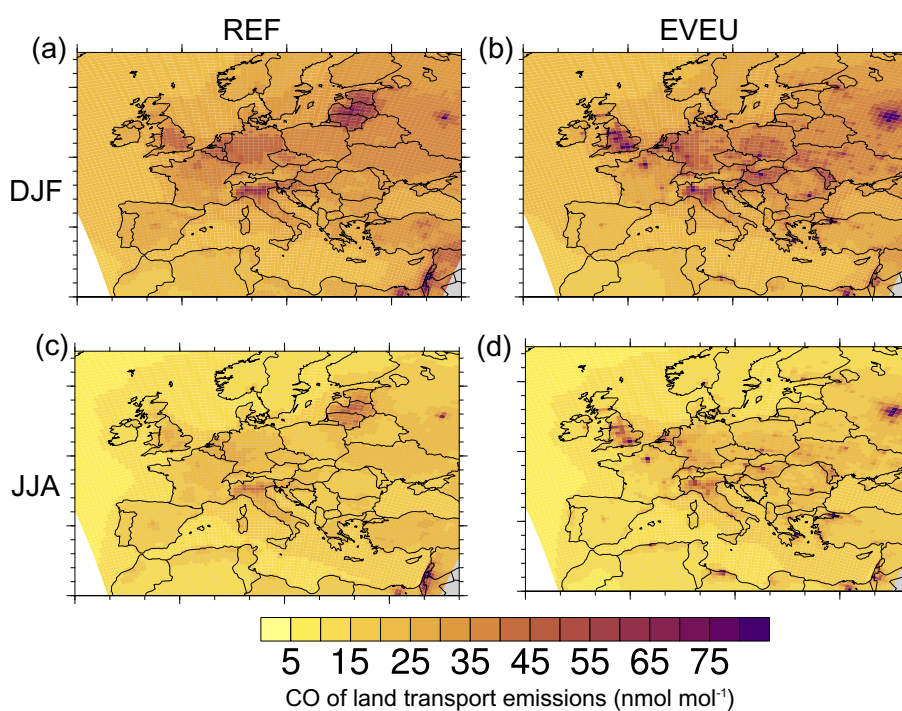Discussions

Figure 4. Absolute contribution of land transport emissions to ground-level CO (in $\mathrm{nmol\,mol^{-1}}$) as simulated by CM50. (a) and (b) contributions for the period DJF of the *REF* and *EVEU* simulations, respectively. (c) and (d) contributions for the period JJA of the *REF* and *EVEU* simulations, respectively.
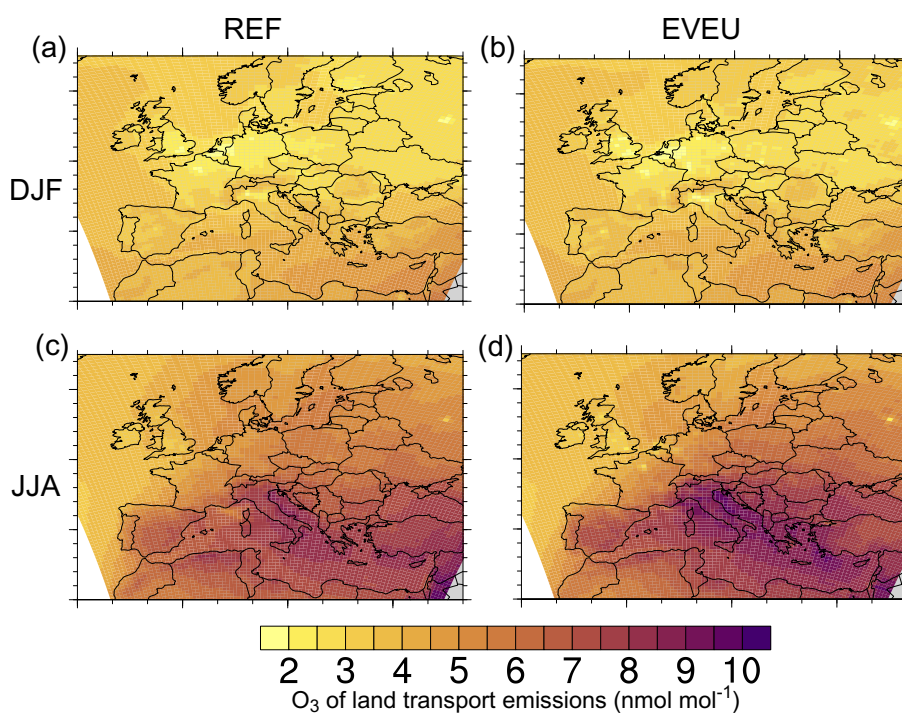
Figure 5. Absolute contribution of land transport emissions to ground-level O_3 (in $nmol\ mol^{-1}$) as simulated by CM50. (a) and (b) contributions for the period DJF of the *REF* and *EVEU* simulations, respectively. (c) and (d) contributions for the period JJA of the *REF* and *EVEU* simulations, respectively.

4   Contributions of land transport emissions to ozone

In difference to NO_y and CO, ozone is a secondary pollutant of the land transport sector. This section quantifies the contribution to ozone in detail. Besides land transport emissions, however, many other sources contribute to ozone near ground level. Generally, the most important sources which contribute globally to ozone are downward transport from the stratosphere,

5   anthropogenic non-traffic emissions, shipping, lightning and biogenic emissions (e.g. Lelieveld and Dentener, 2000; Grewe, 2004; Hoor et al., 2009; Dahlmann et al., 2011; Emmons et al., 2012; Grewe et al., 2017). Table 6 lists the contributions of different emission sources to ozone for Europe averaged for JJA 2008 and for the results of *EVEU* and *REF* (see also Fig. S6 for zonally averaged vertical profiles of the contributions) Near ground level in Europe the most important sources for ozone are biogenic emissions (≈ 19 %), anthropogenic non-traffic (≈ 16 %), methane degradation (≈ 14 %) and land transport (≈ 12 %).

10   With increasing height the contribution of ground based emission sources decreases, therefore the contribution of land transport emission decrease to ≈ 8 %. At the same time the importance of ozone transported downward from the stratosphere, lightning and aviation increases. At a height of 200 hPa more than 50 % of the ozone is from stratospheric origin. The contribution of land transport emissions drops to around 3 %. Further, the differences between the results of *REF* and *EVEU* decrease with increasing height, indicating the larger importance of long range transport which are equal in both simulations due to identical

15   emissions for the global models and therefore identical boundary conditions for CM50.

4.1   Seasonal average contribution to ground-level ozone

During DJF O_3^{tra} simulated by *REF* and *EVEU* (see Fig. 5) ranges between 2 nmol mol^{-1} to 4 nmol mol^{-1}. Due to ozone titration the absolute contributions near some hot-spots are lower than these contributions. These absolute contributions correspond to relative contributions of O_3^{tra} to ground level ozone of around 8 % over large parts of Europe (see Fig. 6). Although the

20   European emission inventories differ, the simulated contributions (absolute as well as relative) show almost no differences. The emissions of the global model, however, are identical in *REF* and *EVEU* leading to identical contributions at the boundaries of the regional domain. Hence, the contributions during DJF are mainly dominated by long range transport towards Europe which has also been reported by Karamchandani et al. (2017). This is caused by the low ozone production and long lifetime of ozone during winter.

25   During summer the ozone production increases and local emissions play a larger role. Therefore, O_3^{tra} increases to 5 to 10 nmol mol^{-1}, implying that the relative contribution increases to 10 to 16 %. The geographical distribution of the contribution are similar for both emission inventories, showing increasing absolute and relative contributions from North-West to South-East. The largest relative contributions are simulated around the Po Valley while the largest absolute contributions are shifted downwind of Italy into the Adriatic Sea. In these regions the differences between the results of the two simulations

30   are largest, reaching up to 2 nmol mol^{-1} for the absolute and 2 percentage-points for the relative contributions, respectively. The larger differences between the results of *REF* and *EVEU* during summer compared to winter are mainly caused by the increasing ozone production over Europe during spring and summer. Accordingly, the differences of the emissions between the emission inventories modify the regional ozone budgets more efficiently.

As already discussed the emission of the land transport sector show almost no annual cycle (Fig S4 in the Supplement), while the absolute and relative contribution of O_3^{tra} shows an annual cycle. This annual cycle is caused by a complex interplay of the annual cycles of different emission sources. The annual cycle of the relative contribution of O_3^{tra} is shown in Fig. 7. The annual cycle of the absolute contribution is similar to the cycle of the relative contribution, but shows the largest peak during

5 June where the absolute ozone levels are larges (See Fig. S9 in the Supplement). Accordingly, the contribution peaks between May to July and in October (≈ 13 % averaged over Europe for the column up to 850 hPa) and has a minimum of 9 % during December to March. The decrease of the contribution during the summer month is mainly caused by the large contribution of biogenic emissions (biogenic VOCs and soil-NO_x) during July and August. Important contributors to the lower contributions during winter are the categories stratosphere and industry showing a strong annual cycle with peaks of the contributions during

10 March and May (Fig. S3 in the Supplement). Further, the indicated standard deviation of the contribution shows that in winter, spring, and autumn the year to year variability (blue shading) is the most important source of uncertainty. Here, differences in regional emission lead only to small differences (orange shading). During summer, however, the differences of the regional emissions strongly contribute to the uncertainties.

The differences between the extreme absolute and relative contributions of O_3^{tra} between *REF* and *EVEU* (expressed as 95th

15 percentile) are larger as for the mean values. The 95th percentile of the relative contribution of O_3^{tra} to ground level ozone reaches up to 24 % in the Po Valley using the VEU emission inventory (see Fig. 8). The maxima applying the MAC emission inventory are lower by 4 to 5 percentage points. In contrast to the mean values, the extreme values occur mainly near the regions with the largest land transport emissions, namely over France, Italy and Germany. Over France and Germany extreme values (depending on the applied emission inventory) between 16 to 18 % occur, while the values in Northern Italy range from

20 20 to 24 %.

Focussing on Germany, the relative contribution of O_3^{tra} to ground level ozone is 10 to 15 %. The contribution has a North-West to South-East gradient. One important contributor to this gradient are the strong shipping emissions in the English Channel, North- and Baltic- sea (e.g. Matthias et al., 2010). These emissions lead to larger relative and absolute contributions of shipping emissions in Northern and Western Germany, which decrease towards the South. The absolute contributions are

25 around 2 to 3 $\mathrm{nmol\,mol^{-1}}$ during DJF and 4 to 6 $\mathrm{nmol\,mol^{-1}}$ during JJA (averaged for 2008 to 2010). The largest 95th percentile of the relative contribution of land transport emissions are simulated in Southern Germany (up to 22 %).
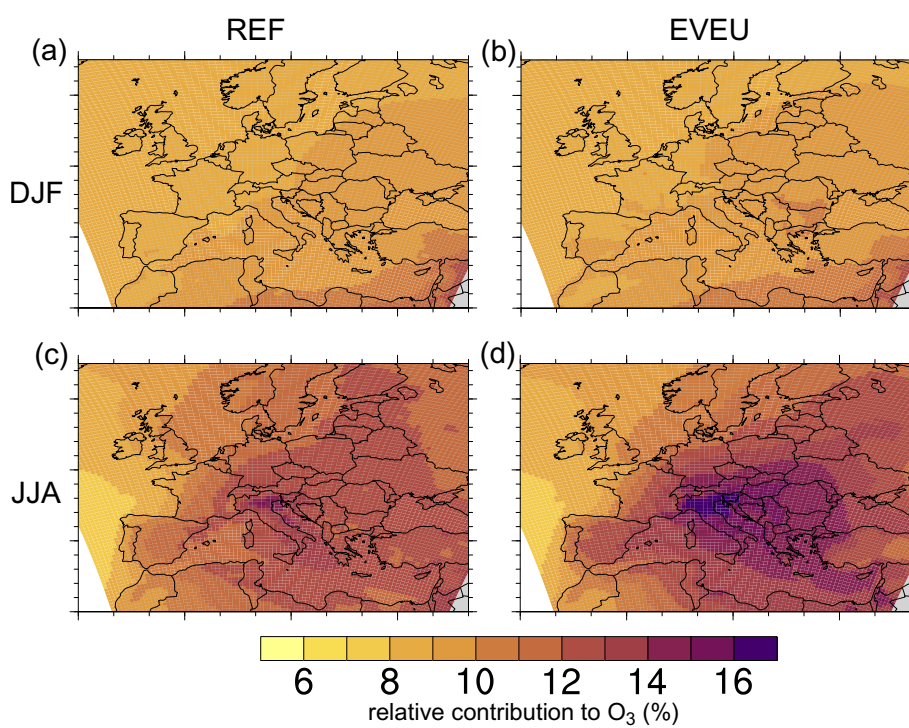
Atmospheric
Chemistry
and Physics
Discussions
Open Access
EGU

Figure 6. Relative contribution of land transport emissions to ground-level O$_3$ (in %) as simulated by CM50. (a) and (b) contributions for the period DJF of the *REF* and *EVEU* simulations, respectively. (c) and (d) contributions for the period JJA of the *REF* and *EVEU* simulations, respectively.
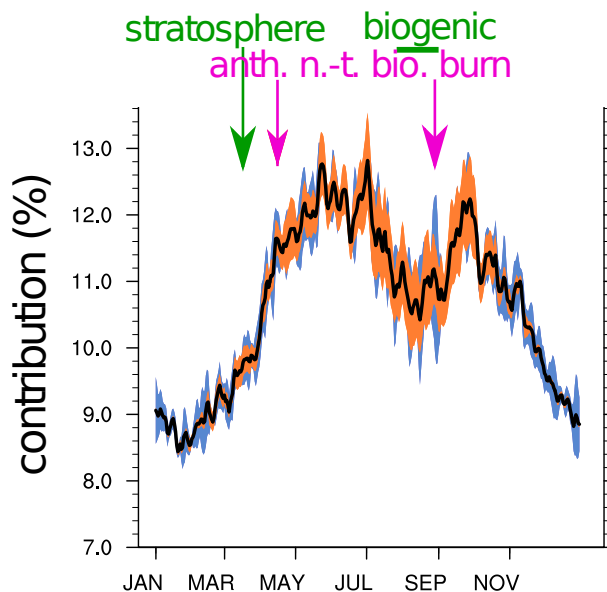
Figure 7. Annual cycle of the relative contribution of land transport emissions to the ozone column up to 850 hPa (in %).The black line indicates the mean contribution as simulated by CM50, averaged over the years 2008–2010 and the two simulations (*REF*, *EVEU*). The blue shading indicates the standard deviation with respect to time for the years 2008 to 2010 for the *EVEU* simulation. The orange shading indicates the standard deviation with respect to time between the 2008–2010 averaged annual cycles between the *REF* and the *EVEU* simulation. The coloured arrows indicate the time frames where specific emission categories (stratosphere, anthropogenic non-traffic, biomass burning, and biogenic) have their largest relative contributions. The category biogenic peaks over a wide range, therefore a bar is used instead of the arrow.
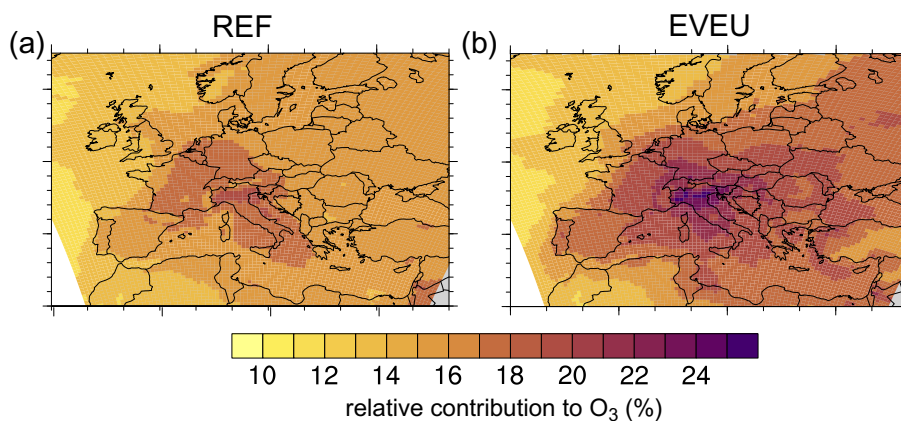

Figure 8. 95th percentile of the relative contribution as simulated by CM50 of land transport emissions to ground-level O_3 (in %) based on 3-hourly model output. (a) and (b) contributions for the period JJA of the *REF* and *EVEU* simulations, respectively.

4.2 Contribution during extreme ozone events

To design mitigation options for periods with extreme ozone values, it is important to know which emission sources contribute to and/or drive these extreme ozone values. Therefore, we investigate how land transport emissions contribute to extreme ozone events.

5   First, the 99th, 95th and 75th percentile of ozone concentration of the period JJA 2008 to 2010 are calculated (based on 3-hourly model output, see Figs. S1 and S2 in the Supplement). Second, the sectors contributing to these 99th, 95th and 75th percentile of ozone are analysed. Generally, the contributions to these extreme values have a high spatial variability. To capture these spatial variability, the contributions are analysed for the whole CM50 domain as well as for specific regional subdomains for which we use the regions defined in the PRUDENCE project (Christensen et al., 2007, , see also Supplement Fig. S10)

10   The range of contributions in the different subdomains is shown in Fig. 9. Generally, the relative contributions of O_3^{tra} (Fig. 9a and b) increase for increasing ozone percentiles in most regions. This increase is largest in the regions Alps (including the Po Valley), Mid Europe, France and the British Islands. The largest contributions of O_3^{tra} occur in the Mediterranean region, the Alps, Mid Europe and France. Especially in these regions, *EVEU* simulates larger median and maximum relative contributions of O_3^{tra} compared to *REF*. Further, the range of contributions for almost all regions is larger in *EVEU* compared 15   to *REF*. This indicates the large influence of the emission inventory uncertainties on the analysis of extreme ozone events. Accordingly, these uncertainties must kept in mind when designing mitigation option for extreme ozone events.

   For the 99th percentile of ground level ozone the median of the relative contributions of O_3^{tra} in the region Alps is around 16 % / 22 % (*REF*/*EVEU* simulation), while the 95th percentile is around 19 % / 24 %. The region with the second largest contributions is Mid Europe (including mainly Germany and the Benelux States). Here, median contributions (at 99th percentile 20   of ozone) of 16 % / 18 % and contributions (at 95th percentile) of 18 % / 22 % are simulated. The largest contributions (between 24 and 28 % for the *EVEU* simulation) are mainly simulated in the Po Valley, in South-Western Germany, Western Germany and around Paris. For the lower percentile of ground level ozone the contributions of land transport emissions decrease and reach median contributions of 13 to 16 % and 95th percentiles of 15 to 21 % in the regions Mediterranean, Alps, Mid Europe and France.

25   The medians of the relative contribution of other anthropogenic emissions (including the emission sectors anthropogenic non-traffic and aviation) range in all regions between 17 % to 25 % (Fig. 9c and d). Hence, the contribution of other anthropogenic emissions is larger as the contribution of land transport emissions. The increase of the contribution of other anthropogenic emissions with increasing ozone percentiles, however, is lower compared to the contribution of O_3^{tra}. Accordingly, the relative importance of land transport emissions increase with increasing ozone values and hence land transport emissions 30   are an important driver of large ozone values. However, besides the land transport emissions also the relative contribution of biogenic emissions to ozone increases with increasing ozone levels (Fig. 9e and f). Therefore, also biogenic emissions play an important role during high ozone values.

   While the relative contribution to ozone of the shown emission sectors increase with increasing ozone levels, the contribution of the shipping emissions and all other emission sectors decrease with increasing ozone levels in all most all regions (Fig. S5

in the Supplement). Only in the Mediterranean region *REF* simulates also an increase of the relative contribution of shipping emissions with increasing ozone levels.
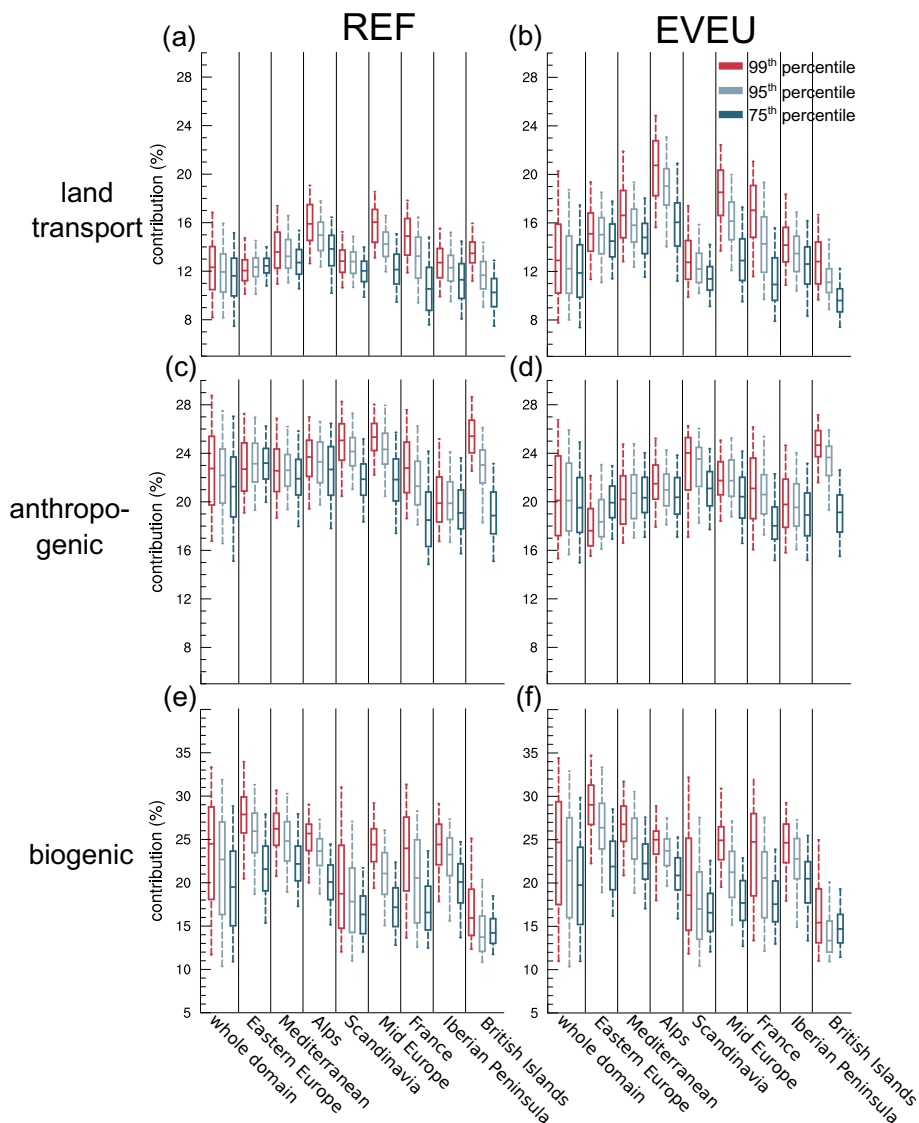
Figure 9. Box-whisker plot showing the contribution of the most important emission sources as simulated by CM50. For simplicity only the contributions for land transport emissions, biogenic emissions and other anthropogenic emissions (anthropogenic non-traffic, and aviation) to ground-level ozone (in %) are shown. Therefore, the contributions do not add up to 100 %. (a) and (b) show the relative contributions of O_3^{tra} at the 99th,95th and 75th percentile of ozone; (c) and (d) the relative contribution of anthropogenic emissions (anthropogenic non-traffic and aviation) at the 99th,95th and 75th percentile of ozone ; and (e) and (f) the relative contribution of O_3^{soi} at the 99th,95th and 75th percentile of ozone. The lower and upper end of the box indicates the 25th and 75th percentile, the bar the median, and the whiskers the 5th and 95th percentile of the contributions of all gridboxes within the indicated regions. All values are calculated for JJA of the period 2008 to 2010 and are based on 3-hourly model output. The data were transformed on a regular grid with a resolution of $0.5°$ x $0.5°$ to allow for the analyses on the defined regions.
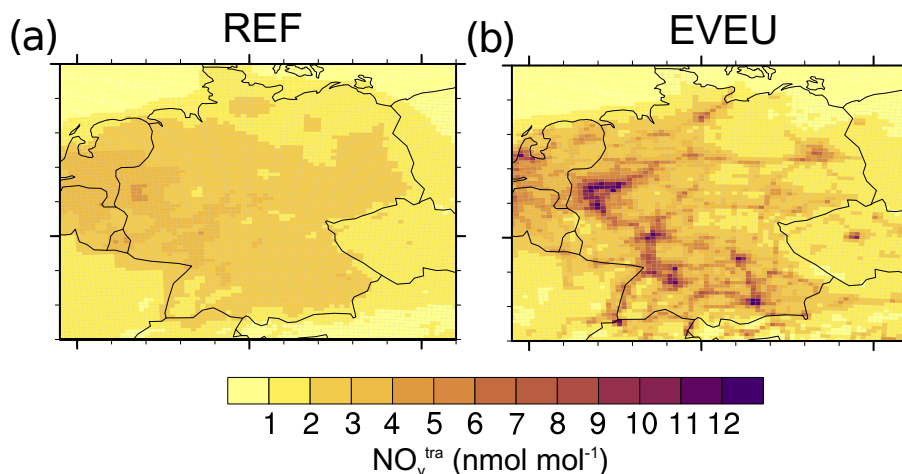
Figure 10. Absolute contribution for JJA 2008 of land transport emissions to all reactive nitrogen (NO_y^{tra}, in nmol mol^{-1} as simulated by CM12. (a) and (b) show contributions for the period JJA of the *REF* and *EVEU* simulations, respectively.

5 Contribution of land transport emissions to reactive nitrogen in Germany

So far the contributions have been analysed using the results of the European domain. The resolution of the VEU emission inventory, however, is much finer (roughly 7 km) and therefore the full potential of the emission inventory has not been revealed. Therefore, this section is dedicated to the results of CM12 focusing on Germany. As shown by Mertens et al. (2019) the contributions of land transport emissions to ozone in Germany change only slightly, when the model resolution is increased from 50 km to 12 km. The differences caused by the resolution are lower as the differences between the *REF* and *EVEU* simulation results. Therefore, we focus on the contributions of land transport emissions to NO_y where the results depend stronger on the model resolution. Figure 10 shows the absolute contribution of NO_y^{tra} for JJA 2008 as simulated by CM12. As already discussed, the differences between the two emission inventories are rather large. The *REF* simulation results show maximum contributions of around 5 nmol mol^{-1}, while the *EVEU* simulation results show contributions of up to 12 nmol mol^{-1}. These large values occur around the large cities in Bavaria (Munich, Nuremberg) and the large cities in (South-)Western Germany (Stuttgart, Frankfurt, Rhine-Ruhr area).

6 Contribution of land transport emissions to the tropospheric ozone budget in Europe

To investigate the contribution of land transport emissions to the European ozone budget the net ozone production (P_{O3}) is analysed which is defined as:

$$P_{O3} = ProdO3 - LossO3, \tag{3}$$

with production (ProdO3) and loss rates (LossO3) of ozone as diagnosed by the tagging method for the different tagged categories (see Grewe et al., 2017).

Our analysis shows (see Table 7) that the land transport sector is the second important anthropogenic sector contributing to P_{O3} in Europe. In general, the results obtained with both emission inventories are rather similar, caused by similar total

5 emissions. Integrated up to 850 hPa values of P_{O3} due to land transport emissions of around 13 $Tg(O_3)\,a^{-1}$ ozone are simulated, while P_{O3} increase to around 23 $Tg(O_3)\,a^{-1}$ when integrating up to 200 hPa.

The differences of the contributions of O_3^{tra} discussed in Sect. 4 are mainly caused by the differences of the total emissions of the anthropogenic non-traffic sector. The diagnosed net production for the anthropogenic non-traffic category differs by roughly 30 % between *REF* and *EVEU*, while the total net ozone production differs by roughly 15 %, i.e. due to the lower total

10 emissions in the VEU emission inventory compared to the MAC inventory less ozone is produced.

The regions where ozone is predominantly formed by land transport emissions is displayed in Fig. 11a and Fig. 11b, showing the relative contribution of land transport emissions to P_{O3}. Here, the analysis is restricted to the period May to September where P_{O3} is largest. Additionally, Fig. 11c and Fig. 11d indicate the emission sectors which contribute most to P_{O3} up to 850 hPa in the respective gridbox. Consistent with previous analyses the results show that the relative contribution of land

15 transport emissions to P_{O3} is in general larger in *EVEU* compared to *REF*. The contribution is lowest in the Atlantic and along the main shipping routes in the Mediterranean Sea. In these regions ozone within the boundary layer is mainly formed from shipping emissions (Fig. 11c and d). Generally, the contribution of land transport emissions to P_{O3} is largest over Central Europe, including parts of the Iberian Peninsula, the British Islands and Italy. In these regions the contributions range from 25 % to 35 % in *REF* and 25 % to 40 % in *EVEU*. Further, the regions of large contributions extend much more to the East

20 (including Austria and Hungry) in *EVEU* compared to *REF*. Besides these regions the contributions range from 15 % to 20 % in most regions. However, both simulation results indicate regions especially in Northern Europe, but also in the Mediterranean Sea and Africa with very large contributions (above 35 %). These regions, however, generally show low absolute values of P_{O3}. Therefore, the large contributions of land transport emissions are not very meaningful. With contributions from 25 % to 40 % land transport emissions are clearly an important contribution to the ozone production up to 850 hPa. However, in only very

25 few regions (Western Germany, Austria and Northern Italy) and only in *EVEU* land transport emissions are the most important contributor to P_{O3} (Fig. 11).

Outside these regions the results of *REF* and *EVEU* show that biogenic emissions are most important over the Iberian Peninsula and over large parts of Eastern Europe as well as over Africa. For Central Europe and Northern Europe the *REF* results indicate that the anthropogenic non-traffic sector is most important, while *EVEU* indicated biogenic and land transport as

30 being most important. Again, this clearly shows that the uncertainty of such analysis is strongly influenced by the uncertainties of the anthropogenic and biogenic emission inventories (or parametrizations to calculate these emissions).
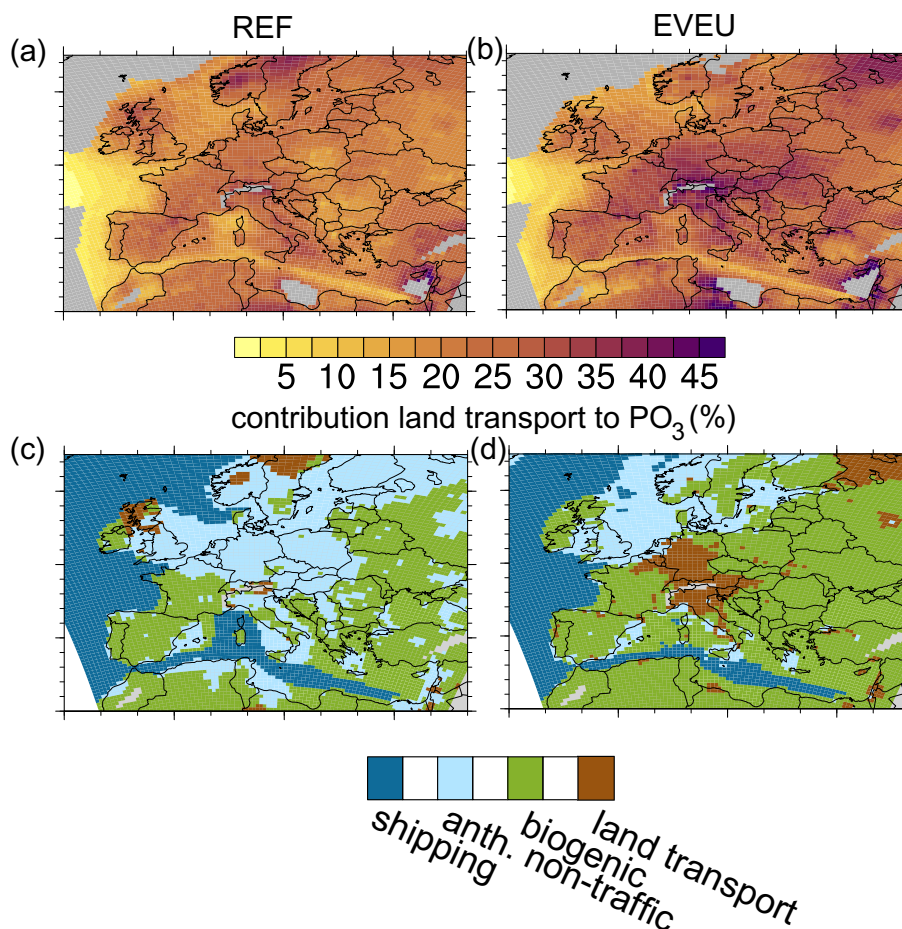
Figure 11. Contribution analysis for P_{O3} from the surface up to 850 hPa. (a) and (b) shows the relative contribution of land transport emissions to P_{O3} (in %) for the *REF* (a) and the *EVEU* (b) simulation. (c) and (d) indicate the emission sector which contributes most to P_{O3} up to 850 hPa, for the *REF* and *EVEU* simulation, respectively. Analysed are averaged data for the period May–September 2008 to 2010 as simulated by CM50. Grey areas in (a) and (b) indicate regions where P_{O3} is below $1.5 \cdot 10^{-13}$ mol mol s^{-1}.

7 Discussion

Our analyses demonstrates the importance of land transport emissions to European reactive nitrogen (NO_y) concentrations. The largest contribution of land transport emissions to NO_y are simulated in Southern England, Benelux, Rhine-Ruhr, Paris and the Po Valley. These regions corresponds well with the regions where ground-level measurements, satellite observations or air-quality simulations report the largest nitrogen dioxide levels (e.g. Curier et al., 2014; Vinken et al., 2014b; Terrenoire et al., 2015; Geddes et al., 2016; European Environment Agency, 2018). Even tough, the absolute contribution (5 to 10 $nmol mol^{-1}$) of land transport emissions to NO_y in these regions strongly depend on the applied emission inventory the relative contributions are 50 % and more. Accordingly, land transport emissions are one of the most important contributor to NO_y in regions with large NO_2 concentrations.

These large amounts of NO_x emissions from land transport clearly contribute to the formation of ozone, but the relative contributions to ozone are lower as the contributions to NO_y. Here, the mean contributions range between 10 % and 16 % in most regions and even during extreme ozone events the contributions are below 25 %. Clearly, land transport emissions are an important contributor to European ozone levels, but they are not the most important contributor to European ozone levels. This is underlined by our analysis of the contribution of land transport emissions to ozone production in Europe, which range between 20 % to 40 % in most areas. The emission sectors which are most important for ozone production in Europe are biogenic emissions as well as anthropogenic non-traffic emissions. During periods of large ozone values, however, our analyses show that the contribution of land transport emissions to ozone increase strongly, while the contribution of anthropogenic non-traffic emissions is only slightly changed. Therefore, land transport emissions contribute strongly to large ozone levels.

We find that the regions of the largest contributions of land transport emissions to ozone are not necessarily identical with the regions of the largest contributions to reactive nitrogen. The ozone values mainly peak in Northern Italy (around the Po Valley) and Southern Germany, which is consistent with the findings of Tagaris et al. (2015). Especially for the Po Valley ground level measurements show that this is one of the regions in Europe with the largest largest ozone levels (e.g. Martilli et al., 2002; Guerreiro et al., 2014; European Environment Agency, 2018). In the regions of Southern England, around Paris, and the Benelux as well as Rhine-Ruhr regions, where the contribution of land transport emissions to NO_y stands out, the contribution to ozone are not largest. This is caused by the complexity and non-linearity of ozone chemistry, which depends not only on the amount of ozone precursors but also on the meteorological conditions (e.g. Monks et al., 2015).

In general our findings with respect to the contributions of land transport emissions to ozone are in agreement with previous studies either using the perturbation method (Tagaris et al., 2015) or a tagging method (Valverde et al., 2016; Karamchandani et al., 2017). In detail, however, previously reported values have been slightly larger. Tagaris et al. (2015) found impacts of up to 20 % in Northern Italy and Southern Germany, and (Valverde et al., 2016) and Karamchandani et al. (2017) report values in the range of 11 to 25 % for most European cities (only for Budapest Karamchandani et al. (2017) reported even larger values of up to 35 %). Compared to these values, however, it is important to note that we investigate the effect of global land transport emissions to European ozone values, while the previous studies investigate only effects due to regional emissions and do not attribute contributions of e.g. land transport emissions in North America. Further, in all studies different emissions, different

ozone metrics, simulation periods and most importantly different analysis methods are used. Previous publications have applied the CMAQ-ISM method (Valverde et al., 2016) or the CAMx OSAT method (Karamchandani et al., 2017). These two methods apply a sensitivity approach to check, if ozone production is NO_x or VOC limited. Depending on this limit ozone production is attributed only to NO_x or VOC emissions. The tagging approach of Grewe et al. (2017) used in this study takes competing

5 effects into account and always attributes ozone production to the sectors of all reaction partners (e.g. NO_x and HO_2 or NO_x and VOC).

The comparison of the results for the two emission inventories sheds light on the uncertainties associated with such a source apportionment method. The differences of the results for the direct pollutants CO and NO_y are rather large. The mean ozone contributions are much less influenced as the direct pollutants. Especially during winter and in the middle/upper troposphere

10 the contributions are mainly dominated by long range transport (e.g. land transport emissions from the rest of the world). In our study, however, we focused on effects only due to European emissions. Therefore, we did not investigate the influence of uncertainties from emissions from the rest of the world. Uncertainties of these emissions are likely to influence the contribution from long range transport.

While the mean values of ozone are only slightly influenced, the analysis of extreme values and the analysis of the emission

15 sectors which are most important for regional ozone production differ largely between the different inventories, even tough the total land transport emissions between the two emission inventories are similar. The differences are mainly caused by the differences of the anthropogenic non-traffic and the shipping emissions between the two emission inventories. Accordingly, the source attribution of land transport emissions is not only influenced by the uncertainties of the land transport emissions itself, but also by the uncertainties of all other emission sectors. As an example, Kuik et al. (2018) reported an underestimation

20 of road traffic emissions for Berlin of up to 50 %. The impact of such large underestimations on the source attribution results have to be investigated. Besides the uncertainties of the land transport and other anthropogenic emissions, especially the emissions of the biogenic sector contribute largely to ozone production in Europe. Accordingly, uncertainties in the biogenic emissions contribute to the analysis of this study. In this context especially the soil-NO_x emissions play an important role as the uncertainties of these emissions are rather large (Vinken et al., 2014a) and the emissions applied in our model system are

25 at the lower end of current emission estimates. Generally, uncertainties caused by the emissions are larger as the uncertainties, which are caused by the simplifications applied in our source apportionment method, which are in the order of some percent (see also discussion by Mertens et al., 2018). Further, our results indicate a large seasonal variability of the contribution of land transport emissions to ozone. This variability is not only caused by the meteorological conditions but also by the seasonal cycle of other emissions. Accordingly, not only the total emissions of different emission sectors but also their seasonality (and

30 the correct representation of this seasonality) plays an important role.

8 Conclusions

In the present study we investigate the contributions of land transport emissions to pollutants in Europe and Germany, focusing on ozone (O_3), carbon monoxide (CO) and reactive nitrogen (NO_y) species by means of simulations with the MECO(n)

model system. This model system couples a global chemistry-climate model on-line with a regional chemistry-climate model To quantify the contributions of land transport emissions to these species we used a tagging method for source apportionment. This tagging method is an accounting system, which completely decomposes the budgets of ozone and ozone precursors into contributions from different emission sources. For the first time such a method is applied consistently in the global as well as

5 the regional models to attribute the emissions of land transport to ozone and ozone precursors. To consider the uncertainties associated with the emission inventories, we performed simulations with two different emission inventories for Europe.

The contribution of land transport emissions to ground level NO_y depends strongly on the applied emission inventory. In general the contributions range from 5 to 10 $nmol\,mol^{-1}$ near the European hotspot regions, which are Western and Southern Germany, the Po Valley, Southern England as well as the Paris and Moscow metropolitan region. In most other parts in Central

10 and Southern Europe contributions of around 2 to 3 $nmol\,mol^{-1}$ are simulated. Generally, absolute contributions during winter are larger as during summer, but the seasonal differences are smaller as the differences by different emission inventories. The absolute contributions correspond to relative contributions of 50 to 70 % to ground-level NO_y, which indicates that land transport emissions are one of the most important sources for NO_y near ground level.

Similar as for NO_y the simulated contributions of land transport emission to CO near ground level depend strongly on

15 the applied emission inventory. Generally, the contributions range between around 30 $nmol\,mol^{-1}$ during summer in regions which are not directly associated with large land transport emission sources and contributions of more than 75 $nmol\,mol^{-1}$ near emission hot spots such as Paris or Moscow.

The contribution of land transport emissions to ozone, which is a secondary pollutant, shows a geographical distribution which differ strongly from the distribution of the primary emissions. The absolute contribution shows a strong North-West

20 South-East gradient with the largest contributions around the Mediterranean Sea. Due to the non-linear behaviour of ozone chemistry and the strong dependency of ozone formation on the meteorology and other precursors as NO_x, regions with large emissions in Western Europe (Benelux, British Islands, Western Germany) show no peak of the contribution of land transport emissions to ozone. This peak is simulated in the Po Valley, where large emissions and favourable conditions for ozone production are present. Generally, the contribution has a strong annual cycle with values of 2 to 3 $nmol\,mol^{-1}$ during

25 winter and 5 to 10 $nmol\,mol^{-1}$ during summer. These absolute contributions correspond to relative contributions between 8 to 16 %. During winter, the results obtained for the two European emission inventories show almost no differences. The contributions are largely determined by long range transport and the inter annual variability is the largest source of uncertainty. Of course also uncertainties of the emission inventories outside Europe play an important role for the uncertainties, but this role has not be investigated in the present study. During summer the differences between the two emission inventories are

30 larger as the inter annual variability and hence uncertainties of emission inventories contribute strongly to the uncertainties of the contribution analysis of land transport emissions to ozone. While the emission of the land transport sector have almost no seasonal cycle, the strong seasonal cycle of the contribution of these emissions to ozone show the strong influence of other emission sources on the ozone production from land transport emissions. Hence, uncertainties in the totals, geographical distributions and the seasonal cycle of other emissions strongly influence the contribution analysis of land transport emissions.

Especially during summer one key role are the biogenic emissions. The impact of uncertainties of these emissions need to be studies in more detail.

The contributions of land transport emissions to extreme (99th percentile) ozone values is largest in the Po Valley, reaching up to roughly 25 %. In other regions of Europe the contributions of land transport emissions to extreme ozone events are lower and strongly depend on the region and the emission inventory. Important is, however, that the contribution of land transport emissions to ozone increase with increasing ozone levels. This indicates that land transport emissions play an important role for high ozone events. Generally, the land transport emissions contribute to the ozone production up to 850 hPa to 20 and 40 % in most European regions. However, only in very few regions land transport emissions are the most important contributions o the ozone production. In most region anthropogenic non-traffic and biogenic emissions are more important. Our analysis shows that especially the biogenic emissions are also important during high ozone events as the contribution of biogenic emissions increase with increasing ozone levels similar to the contribution of land transport emissions. The contributions of anthropogenic non-traffic emissions show almost no increase. However, the large differences obtained for the two emission inventories indicate a large uncertainty range of such analysis.

As a next step the performed analysis will be refined using a source apportionment, which differentiate between contributions of European land transport emissions and land transport emissions from the rest of the world. Such an analysis will help to quantify the importance of European and global land transport emissions, to ozone levels in Europe. Further, more reliable emission estimates are important for follow up studies. Here, the focus should not only be on the land transport emissions, but also on other important emissions, including especially biogenic and soil-NO_x emissions, which have large uncertainties and contribute strongly to European ozone levels. To better constrain the uncertainties of the contribution analysis follow up studies are planned in which we will combine observational data of specific aircraft measurement campaigns together with model results including the analysed contributions.

Code and data availability. The Modular Earth Submodel System (MESSy) is continuously further developed and applied by a consortium of institutions. The usage of MESSy and access to the source code is licenced to all affiliates of institutions which are members of the MESSy Consortium. Institutions can become a member of the MESSy Consortium by signing the MESSy Memorandum of Understanding. More information, including on how to become licensee for the required third party software, can be found on the MESSy Consortium Website (http://www.messy-interface.org). The simulations performed here has been based on MESSy version 2.50 and is available in the official release (version 2.51). The namelist set-up used for the simulations is part of the electronic supplement. The data used for the figures will be part of the electronic supplement once the manuscript is accepted for final publication.

Author contributions. MM performed the simulations, analysed the data and drafted the manuscript. AK and PJ developed the model system. VG developed the tagging method. RS drafted the study. All authors contributed to the interpretation of the results and to the text.

Competing interests. The authors declare that they have no competing interests.

References

Aulinger, A., Matthias, V., Zeretzke, M., Bieser, J., Quante, M., and Backes, A.: The impact of shipping emissions on air pollution in the greater North Sea region – Part 1: Current emissions and concentrations, Atmospheric Chemistry and Physics, 16, 739–758, https://doi.org/10.5194/acp-16-739-2016, http://www.atmos-chem-phys.net/16/739/2016/, 2016.

5 Christensen, J. H., Carter, T. R., Rummukainen, M., and Amanatidis, G.: Evaluating the performance and utility of regional climate models: the PRUDENCE project, Climatic Change, 81, 1–6, https://doi.org/10.1007/s10584-006-9211-6, http://dx.doi.org/10.1007/s10584-006-9211-6, 2007.

Clappier, A., Belis, C. A., Pernigotti, D., and Thunis, P.: Source apportionment and sensitivity analysis: two methodologies with two different purposes, Geoscientific Model Development, 10, 4245–4256, https://doi.org/10.5194/gmd-10-4245-2017, https://www.geosci-model-dev.net/10/4245/2017/, 2017.

Crippa, M., Guizzardi, D., Muntean, M., Schaaf, E., Dentener, F., van Aardenne, J. A., Monni, S., Doering, U., Olivier, J. G. J., Pagliari, V., and Janssens-Maenhout, G.: Gridded emissions of air pollutants for the period 1970–2012 within EDGAR v4.3.2, Earth System Science Data, 10, 1987–2013, https://doi.org/10.5194/essd-10-1987-2018, https://www.earth-syst-sci-data.net/10/1987/2018/, 2018.

Crutzen, Paul, J.: Photochemical reactions initiated by and influencing ozone in unpolluted tropospheric air, Tellus, 26, 47–57, https://doi.org/10.1111/j.2153-3490.1974.tb01951.x, http://dx.doi.org/10.1111/j.2153-3490.1974.tb01951.x, 1974.

Curci, G., Beekmann, M., Vautard, R., Smiatek, G., Steinbrecher, R., Theloke, J., and Friedrich, R.: Modelling study of the impact of isoprene and terpene biogenic emissions on European ozone levels, Atmospheric Environment, 43, 1444 – 1455, https://doi.org/https://doi.org/10.1016/j.atmosenv.2008.02.070, http://www.sciencedirect.com/science/article/pii/S1352231008002124, natural and Biogenic Emissions of Environmentally Relevant Atmospheric Trace Constituents in Europe, 2009.

20 Curier, R., Kranenburg, R., Segers, A., Timmermans, R., and Schaap, M.: Synergistic use of OMI NO2 tropospheric columns and LOTOS–EUROS to evaluate the NOx emission trends across Europe, Remote Sensing of Environment, 149, 58 – 69, https://doi.org/https://doi.org/10.1016/j.rse.2014.03.032, http://www.sciencedirect.com/science/article/pii/S0034425714001321, 2014.

Dahlmann, K., Grewe, V., Ponater, M., and Matthes, S.: Quantifying the contributions of individual NOx sources to the trend in ozone radiative forcing, Atmos. Environ., 45, 2860–2868, https://doi.org/http://dx.doi.org/10.1016/j.atmosenv.2011.02.071, http://www.sciencedirect.com/science/article/pii/S1352231011002366, 2011.

Deckert, R., Jöckel, P., Grewe, V., Gottschaldt, K.-D., and Hoor, P.: A quasi chemistry-transport model mode for EMAC, Geosci. Model Dev., 4, 195–206, https://doi.org/10.5194/gmd-4-195-2011, http://www.geosci-model-dev.net/4/195/2011/, 2011.

Dee, D. P., Uppala, S. M., Simmons, A. J., Berrisford, P., Poli, P., Kobayashi, S., Andrae, U., Balmaseda, M. A., Balsamo, G., Bauer, P., Bechtold, P., Beljaars, A. C. M., van de Berg, L., Bidlot, J., Bormann, N., Delsol, C., Dragani, R., Fuentes, M., Geer, A. J., Haimberger, L., Healy, S. B., Hersbach, H., Hólm, E. V., Isaksen, L., Kållberg, P., Köhler, M., Matricardi, M., McNally, A. P., Monge-Sanz, B. M., Morcrette, J.-J., Park, B.-K., Peubey, C., de Rosnay, P., Tavolato, C., Thépaut, J.-N., and Vitart, F.: The ERA-Interim reanalysis: configuration and performance of the data assimilation system, Quart. J. Roy. Meteor. Soc., 137, 553–597, https://doi.org/10.1002/qj.828, http://dx.doi.org/10.1002/qj.828, 2011.

Degraeuwe, B., Thunis, P., Clappier, A., Weiss, M., Lefebvre, W., Janssen, S., and Vranckx, S.: Impact of passenger car NOX emissions on urban NO2 pollution - Scenario analysis for 8 European cities, Atmospheric Environment, 171, 330 – 337, https://doi.org/https://doi.org/10.1016/j.atmosenv.2017.10.040, http://www.sciencedirect.com/science/article/pii/S1352231017307057, 2017.

Dietmüller, S., Jöckel, P., Tost, H., Kunze, M., Gellhorn, C., Brinkop, S., Frömming, C., Ponater, M., Steil, B., Lauer, A., and Hendricks, J.: A new radiation infrastructure for the Modular Earth Submodel System (MESSy, based on version 2.51), Geoscientific Model Development, 9, 2209–2222, https://doi.org/10.5194/gmd-9-2209-2016, http://www.geosci-model-dev.net/9/2209/2016/, 2016.

Dunker, A. M., Yarwood, G., Ortmann, J. P., and Wilson, G. M.: Comparison of Source Apportionment and Source Sensitivity of Ozone in a Three-Dimensional Air Quality Model, Environmental Science & Technology, 36, 2953–2964, https://doi.org/10.1021/es011418f, http://dx.doi.org/10.1021/es011418f, pMID: 12144273, 2002.

Ehlers, C., Klemp, D., Rohrer, F., Mihelcic, D., Wegener, R., Kiendler-Scharr, A., and Wahner, A.: Twenty years of ambient observations of nitrogen oxides and specified hydrocarbons in air masses dominated by traffic emissions in Germany, Faraday Discuss, https://doi.org/10.1039/C5FD00180C, http://dx.doi.org/10.1039/C5FD00180C, 2016.

Emmons, L. K., Hess, P. G., Lamarque, J.-F., and Pfister, G. G.: Tagged ozone mechanism for MOZART-4, CAM-chem and other chemical transport models, Geosci. Model Dev., 5, 1531–1542, https://doi.org/10.5194/gmd-5-1531-2012, http://www.geosci-model-dev.net/5/1531/2012/, 2012.

European Environment Agency: Air quality in Europe - 2018 report, https://doi.org/10.2800/777411, https://www.eea.europa.eu/publications/air-quality-in-europe-2018/at_download/file, 2018.

Fowler, D., Pilegaard, K., Sutton, M., Ambus, P., Raivonen, M., Duyzer, J., Simpson, D., Fagerli, H., Fuzzi, S., Schjoerring, J., Granier, C., Neftel, A., Isaksen, I., Laj, P., Maione, M., Monks, P., Burkhardt, J., Daemmgen, U., Neirynck, J., Personne, E., Wichink-Kruit, R., Butterbach-Bahl, K., Flechard, C., Tuovinen, J., Coyle, M., Gerosa, G., Loubet, B., Altimir, N., Gruenhage, L., Ammann, C., Cieslik, S., Paoletti, E., Mikkelsen, T., Ro-Poulsen, H., Cellier, P., Cape, J., Horvàth, L., Loreto, F., Niinemets, U., Palmer, P., Rinne, J., Misztal, P., Nemitz, E., Nilsson, D., Pryor, S., Gallagher, M., Vesala, T., Skiba, U., Brüggemann, N., Zechmeister-Boltenstern, S., Williams, J., O'Dowd, C., Facchini, M., de Leeuw, G., Flossman, A., Chaumerliac, N., and Erisman, J.: Atmospheric composition change: Ecosystems-Atmosphere interactions, Atmospheric Environment, 43, 5193–5267, https://doi.org/http://dx.doi.org/10.1016/j.atmosenv.2009.07.068, http://www.sciencedirect.com/science/article/pii/S1352231009006633, ACCENT Synthesis, 2009.

Geddes, J. A., Martin, R. V., Boys, B. L., and van Donkelaar, A.: Long-Term Trends Worldwide in Ambient NO_2 Concentrations Inferred from Satellite Observations, Environmental Health Perspectives, 124, 281–289, https://doi.org/10.1289/ehp.1409567, 2016.

Giorgetta, M. A. and Bengtsson, L.: Potential role of the quasi-biennial oscillation in the stratosphere-troposphere exchange as found in water vapor in general circulation model experiments, J. Geophys. Res. Atmos., 104, 6003–6019, https://doi.org/10.1029/1998JD200112, http://dx.doi.org/10.1029/1998JD200112, 1999.

Granier, C. and Brasseur, G. P.: The impact of road traffic on global tropospheric ozone, Geophys. Res. Lett., 30, https://doi.org/10.1029/2002GL015972, http://dx.doi.org/10.1029/2002GL015972, 2003.

Granier, C., Bessagnet, B., Bond, T., D'Angiola, A., van der Gon, H. D., Frost, G., Heil, A., Kaiser, J., Kinne, S., Klimont, Z., Kloster, S., Lamarque, J.-F., Liousse, C., Masui, T., Meleux, F., Mieville, A., Ohara, T., Raut, J.-C., Riahi, K., Schultz, M., Smith, S., Thompson, A., Aardenne, J., Werf, G., and Vuuren, D.: Evolution of anthropogenic and biomass burning emissions of air pollutants at global and regional scales during the 1980–2010 period, Clim. Change, 109, 163–190, 2011.

Grewe, V.: Technical Note: A diagnostic for ozone contributions of various NO_x emissions in multi-decadal chemistry-climate model simulations, Atmos. Chem. Phys., 4, 729–736, https://doi.org/10.5194/acp-4-729-2004, http://www.atmos-chem-phys.net/4/729/2004/, 2004.

Grewe, V.: A generalized tagging method, Geosci. Model Dev., 6, 247–4253, https://doi.org/10.5194/gmdd-5-3311-2012, http://www.geosci-model-dev-discuss.net/5/3311/2012/, 2013.

Grewe, V., Tsati, E., Mertens, M., Frömming, C., and Jöckel, P.: Contribution of emissions to concentrations: the TAGGING 1.0 submodel based on the Modular Earth Submodel System (MESSy 2.52), Geoscientific Model Development, 10, 2615–2633, https://doi.org/10.5194/gmd-10-2615-2017, https://www.geosci-model-dev.net/10/2615/2017/, 2017.

Guenther, A., Hewitt, C., E., D., Fall, R. G., C., Graedel, T., Harley, P., Klinger, L., Lerdau, M., McKay, W., Pierce, T., S., B., Steinbrecher, R., Tallamraju, R., Taylor, J., and Zimmermann, P.: A global model of natural volatile organic compound emissions, J. Geophys. Res., 100, 8873–8892, 1995.

Guerreiro, C. B., Foltescu, V., and de Leeuw, F.: Air quality status and trends in Europe, Atmospheric Environment, 98, 376 – 384, https://doi.org/https://doi.org/10.1016/j.atmosenv.2014.09.017, http://www.sciencedirect.com/science/article/pii/S1352231014007109, 2014.

Hendricks, J., Righi, M., Dahlmann, K., Gottschaldt, K.-D., Grewe, V., Ponater, M., Sausen, R., Heinrichs, D., Winkler, C., Wolfermann, A., Kampffmeyer, T., Friedrich, R., Klötzke, M., and Kugler, U.: Quantifying the climate impact of emissions from land-based transport in Germany, Transportation Research Part D: Transport and Environment, https://doi.org/https://doi.org/10.1016/j.trd.2017.06.003, 2017.

Hofmann, C., Kerkweg, A., Wernli, H., and Jöckel, P.: The 1-way on-line coupled atmospheric chemistry model system MECO(n) Part 3: Meteorological evaluation of the on-line coupled system, Geosci. Model Dev., 5, 129–147, https://doi.org/10.5194/gmd-5-129-2012, http://www.geosci-model-dev.net/5/129/2012/, 2012.

Holmes, C. D., Prather, M. J., and Vinken, G. C. M.: The climate impact of ship NO_x emissions: an improved estimate accounting for plume chemistry, Atmospheric Chemistry and Physics, 14, 6801–6812, https://doi.org/10.5194/acp-14-6801-2014, http://www.atmos-chem-phys.net/14/6801/2014/, 2014.

Hoor, P., Borken-Kleefeld, J., Caro, D., Dessens, O., Endresen, O., Gauss, M., Grewe, V., Hauglustaine, D., Isaksen, I. S. A., Jöckel, P., Lelieveld, J., Myhre, G., Meijer, E., Olivie, D., Prather, M., Schnadt Poberaj, C., Shine, K. P., Staehelin, J., Tang, Q., van Aardenne, J., van Velthoven, P., and Sausen, R.: The impact of traffic emissions on atmospheric ozone and OH: results from QUANTIFY, Atmos. Chem. Phys., 9, 3113–3136, https://doi.org/10.5194/acp-9-3113-2009, http://www.atmos-chem-phys.net/9/3113/2009/, 2009.

Jöckel, P., Sander, R., Kerkweg, A., Tost, H., and Lelieveld, J.: Technical Note: The Modular Earth Submodel System (MESSy) - a new approach towards Earth System Modeling, Atmos. Chem. Phys., 5, 433–444, https://doi.org/10.5194/acp-5-433-2005, http://www.atmos-chem-phys.net/5/433/2005/, 2005.

Jöckel, P., Tost, H., Pozzer, A., Brühl, C., Buchholz, J., Ganzeveld, L., Hoor, P., Kerkweg, A., Lawrence, M., Sander, R., Steil, B., Stiller, G., Tanarhte, M., Taraborrelli, D., van Aardenne, J., and Lelieveld, J.: The atmospheric chemistry general circulation model ECHAM5/MESSy1: consistent simulation of ozone from the surface to the mesosphere, Atmos. Chem. Phys., 6, 5067–5104, https://doi.org/10.5194/acp-6-5067-2006, http://www.atmos-chem-phys.net/6/5067/2006/, 2006.

Jöckel, P., Kerkweg, A., Pozzer, A., Sander, R., Tost, H., Riede, H., Baumgaertner, A., Gromov, S., and Kern, B.: Development cycle 2 of the Modular Earth Submodel System (MESSy2), Geosci. Model Dev., 3, 717–752, https://doi.org/10.5194/gmd-3-717-2010, http://www.geosci-model-dev.net/3/717/2010/, 2010.

Jöckel, P., Tost, H., Pozzer, A., Kunze, M., Kirner, O., Brenninkmeijer, C. A. M., Brinkop, S., Cai, D. S., Dyroff, C., Eckstein, J., Frank, F., Garny, H., Gottschaldt, K.-D., Graf, P., Grewe, V., Kerkweg, A., Kern, B., Matthes, S., Mertens, M., Meul, S., Neumaier, M., Nützel, M., Oberländer-Hayn, S., Ruhnke, R., Runde, T., Sander, R., Scharffe, D., and Zahn, A.: Earth System Chemistry integrated Modelling (ESCiMo) with the Modular Earth Submodel System (MESSy) version 2.51, Geosci. Model Dev., 9, 1153–1200, https://doi.org/10.5194/gmd-9-1153-2016, http://www.geosci-model-dev.net/9/1153/2016/, 2016.

Jonson, J. E., Schulz, M., Emmons, L., Flemming, J., Henze, D., Sudo, K., Tronstad Lund, M., Lin, M., Benedictow, A., Koffi, B., Dentener, F., Keating, T., Kivi, R., and Davila, Y.: The effects of intercontinental emission sources on European air pollution levels, Atmospheric Chemistry and Physics, 18, 13 655–13 672, https://doi.org/10.5194/acp-18-13655-2018, https://www.atmos-chem-phys.net/18/13655/2018/, 2018.

5 Karamchandani, P., Long, Y., Pirovano, G., Balzarini, A., and Yarwood, G.: Source-sector contributions to European ozone and fine PM in 2010 using AQMEII modeling data, Atmospheric Chemistry and Physics, 17, 5643–5664, https://doi.org/10.5194/acp-17-5643-2017, https://www.atmos-chem-phys.net/17/5643/2017/, 2017.

Kerkweg, A. and Jöckel, P.: The 1-way on-line coupled atmospheric chemistry model system MECO(n) Part 1: Description of the limited-area atmospheric chemistry model COSMO/MESSy, Geosci. Model Dev., 5, 87–110, https://doi.org/10.5194/gmd-5-87-2012, http://www.
10 geosci-model-dev.net/5/87/2012/, 2012a.

Kerkweg, A. and Jöckel, P.: The 1-way on-line coupled atmospheric chemistry model system MECO(n) - Part 2: On-line coupling with the Multi-Model-Driver (MMD), Geosci. Model Dev., 5, 111–128, https://doi.org/10.5194/gmd-5-111-2012, http://www.geosci-model-dev. net/5/111/2012/, 2012b.

Kerkweg, A., Buchholz, J., Ganzeveld, L., Pozzer, A., Tost, H., and Jöckel, P.: Technical Note: An implementation of the dry removal
15 processes DRY DEPosition and SEDImentation in the Modular Earth Submodel System (MESSy), Atmos. Chem. Phys., 6, 4617–4632, https://doi.org/10.5194/acp-6-4617-2006, http://www.atmos-chem-phys.net/6/4617/2006/, 2006a.

Kerkweg, A., Sander, R., Tost, H., and Jöckel, P.: Technical note: Implementation of prescribed (OFFLEM), calculated (ONLEM), and pseudo-emissions (TNUDGE) of chemical species in the Modular Earth Submodel System (MESSy), Atmos. Chem. Phys., 6, 3603–3609, https://doi.org/10.5194/acp-6-3603-2006, http://www.atmos-chem-phys.net/6/3603/2006/, 2006b.

20 Kerkweg, A., Hofmann, C., Jöckel, P., Mertens, M., and Pante, G.: The on-line coupled atmospheric chemistry model system MECO(n) – Part 5: Expanding the Multi-Model-Driver (MMD v2.0) for 2-way data exchange including data interpolation via GRID (v1.0), Geoscientific Model Development, 11, 1059–1076, https://doi.org/10.5194/gmd-11-1059-2018, https://www.geosci-model-dev.net/11/1059/2018/, 2018.

Kuik, F., Kerschbaumer, A., Lauer, A., Lupascu, A., von Schneidemesser, E., and Butler, T. M.: Top–down quantification of NO_x emissions
25 from traffic in an urban area using a high-resolution regional atmospheric chemistry model, Atmospheric Chemistry and Physics, 18, 8203–8225, https://doi.org/10.5194/acp-18-8203-2018, https://www.atmos-chem-phys.net/18/8203/2018/, 2018.

Kwok, R. H. F., Baker, K. R., Napelenok, S. L., and Tonnesen, G. S.: Photochemical grid model implementation and application of VOC, NO_x, and O_3 source apportionment, Geoscientific Model Development, 8, 99–114, https://doi.org/10.5194/gmd-8-99-2015, http://www. geosci-model-dev.net/8/99/2015/, 2015.

30 Landgraf, J. and Crutzen, P. J.: An efficient method for online calculations of photolysis and heating rates., J. Atmos. Sci., 55, 863–878, https://doi.org/http://dx.doi.org/10.1175/1520-0469, 1998.

Lelieveld, J. and Dentener, F. J.: What controls tropospheric ozone?, J. Geophys. Res. Atmos., 105, 3531–3551, https://doi.org/10.1029/1999JD901011, http://dx.doi.org/10.1029/1999JD901011, 2000.

Li, Y., Lau, A. K.-H., Fung, J. C.-H., Zheng, J. Y., Zhong, L. J., and Louie, P. K. K.: Ozone source apportionment (OSAT) to differentiate local
35 regional and super-regional source contributions in the Pearl River Delta region, China, Journal of Geophysical Research: Atmospheres, 117, https://doi.org/10.1029/2011JD017340, http://dx.doi.org/10.1029/2011JD017340, d15305, 2012.

Atmospheric
Chemistry
and Physics
Discussions
Open Access
EGU

Markakis, K., Valari, M., Perrussel, O., Sanchez, O., and Honore, C.: Climate-forced air-quality modeling at the urban scale: sensitivity to model resolution, emissions and meteorology, Atmospheric Chemistry and Physics, 15, 7703–7723, https://doi.org/10.5194/acp-15-7703-2015, https://www.atmos-chem-phys.net/15/7703/2015/, 2015.

Martilli, A., Neftel, A., Favaro, G., Kirchner, F., Sillman, S., and Clappier, A.: Simulation of the ozone formation in the northern part of the Po Valley, Journal of Geophysical Research: Atmospheres, 107, LOP 8–1–LOP 8–20, https://doi.org/10.1029/2001JD000534, https://agupubs.onlinelibrary.wiley.com/doi/abs/10.1029/2001JD000534, 2002.

Matthes, S., Grewe, V., Sausen, R., and Roelofs, G.-J.: Global impact of road traffic emissions on tropospheric ozone, Atmos. Chem. Phys., 7, 1707–1718, https://doi.org/10.5194/acp-7-1707-2007, http://www.atmos-chem-phys.net/7/1707/2007/, 2007.

Matthias, V., Bewersdorff, I., Aulinger, A., and Quante, M.: The contribution of ship emissions to air pollution in the North Sea regions, Environmental Pollution, 158, 2241 – 2250, https://doi.org/https://doi.org/10.1016/j.envpol.2010.02.013, http://www.sciencedirect.com/science/article/pii/S0269749110000746, advances of air pollution science: from forest decline to multiple-stress effects on forest ecosystem services, 2010.

Mauzerall, D. L., , and Wang, X.: Protecting agricultural crops from th effects of tropospheric ozone exposure: Reconciling Science and Standard Setting in the United States, Europe, and Asia, Annu Rev Energ Environ, 26, 237–268, https://doi.org/10.1146/annurev.energy.26.1.237, http://dx.doi.org/10.1146/annurev.energy.26.1.237, 2001.

Mertens, M., Kerkweg, A., Jöckel, P., Tost, H., and Hofmann, C.: The 1-way on-line coupled model system MECO(n) – Part 4: Chemical evaluation (based on MESSy v2.52), Geoscientific Model Development, 9, 3545–3567, https://doi.org/10.5194/gmd-9-3545-2016, http://www.geosci-model-dev.net/9/3545/2016/, 2016.

Mertens, M., Grewe, V., Rieger, V. S., and Jöckel, P.: Revisiting the contribution of land transport and shipping emissions to tropospheric ozone, Atmospheric Chemistry and Physics, 18, 5567–5588, https://doi.org/10.5194/acp-18-5567-2018, https://www.atmos-chem-phys.net/18/5567/2018/, 2018.

Mertens, M., Kerkweg, A., Grewe, V., Jöckel, P., and Sausen, R.: Are contributions of emissions to ozone a matter of scale? – A study using MECO(n) (MESSy v2.50), Geoscientific Model Development Discussions, 2019, 1–23, https://doi.org/10.5194/gmd-2019-7, https://www.geosci-model-dev-discuss.net/gmd-2019-7/, 2019.

Mertens, M. B.: Contribution of road traffic emissions to tropospheric ozone in Europe and Germany, http://nbn-resolving.de/urn:nbn:de:bvb:19-207288, 2017.

Monks, P. S., Archibald, A. T., Colette, A., Cooper, O., Coyle, M., Derwent, R., Fowler, D., Granier, C., Law, K. S., Mills, G. E., Stevenson, D. S., Tarasova, O., Thouret, V., von Schneidemesser, E., Sommariva, R., Wild, O., and Williams, M. L.: Tropospheric ozone and its precursors from the urban to the global scale from air quality to short-lived climate forcer, Atmos. Chem. Phys., 15, 8889–8973, https://doi.org/10.5194/acp-15-8889-2015, http://www.atmos-chem-phys.net/15/8889/2015/, 2015.

Myhre, G., Shindell, D., Breéon, F.-M., Collins, W., Fuglestvedt, J., Huang, J., Koch, D., Lamarque, J.-F, Lee, D., Mendoza, B., Nakajima, T., Robock, A., Stephens, G., Takemura, T., and Zhang, H.: Anthropogenic and Natural Radiative Forcing, pp. 659–740, https://doi.org/10.1017/CBO9781107415324.018, www.climatechange2013.org, 2013.

Niemeier, U., Granier, C., Kornblueh, L., Walters, S., and Brasseur, G. P.: Global impact of road traffic on atmospheric chemical composition and on ozone climate forcing, J. Geophys. Res. Atmos., 111, https://doi.org/10.1029/2005JD006407, http://dx.doi.org/10.1029/2005JD006407, 2006.

Ntziachristos, L., Papadimitriou, G., Ligterink, N., and Hausberger, S.: Implications of diesel emissions control failures to emission factors and road transport NOx evolution, Atmospheric Environment, 141, 542 – 551,

https://doi.org/https://doi.org/10.1016/j.atmosenv.2016.07.036,   http://www.sciencedirect.com/science/article/pii/S1352231016305568,
2016.

Pay, M. T., Gangoiti, G., Guevara, M., Napelenok, S., Querol, X., Jorba, O., and Pérez García-Pando, C.: Ozone source apportionment
during peak summer events over southwestern Europe, Atmospheric Chemistry and Physics, 19, 5467–5494, https://doi.org/10.5194/acp-
19-5467-2019, https://www.atmos-chem-phys.net/19/5467/2019/, 2019.

Peitzmeier, C., Loschke, C., Wiedenhaus, H., and Klemm, O.: Real-world vehicle emissions as measured by in situ analysis of
exhaust plumes, Environmental Science and Pollution Research, 24, 23 279–23 289, https://doi.org/10.1007/s11356-017-9941-1,
https://www.scopus.com/inward/record.uri?eid=2-s2.0-85028012880&doi=10.1007%2fs11356-017-9941-1&partnerID=40&md5=
bfebeef2115b0bf3c935009e2bb6dd44, cited By 1, 2017.

Pöschl, U., von Kuhlmann, R., Poisson, N., and Crutzen, P.: Development and Intercomparison of Condensed Isoprene Oxidation Mecha-
nisms for Global Atmospheric Modeling, J. Atmos. Chem., 37, 29–152, https://doi.org/10.1023/A:1006391009798, http://dx.doi.org/10.
1023/A%3A1006391009798, 2000.

Pozzer, A., Jöckel, P., Sander, R., Williams, J., Ganzeveld, L., and Lelieveld, J.: Technical Note: The MESSy-submodel AIRSEA cal-
culating the air-sea exchange of chemical species, Atmos. Chem. Phys., 6, 5435–5444, https://doi.org/10.5194/acp-6-5435-2006, http:
//www.atmos-chem-phys.net/6/5435/2006/, 2006.

Price, C. and Rind, D.: Modeling Global Lightning Distributions in a General Circulation Model, Monthly Weather Review,
122, 1930–1939, https://doi.org/10.1175/1520-0493(1994)122<1930:MGLDIA>2.0.CO;2, https://doi.org/10.1175/1520-0493(1994)
122<1930:MGLDIA>2.0.CO;2, 1994.

Reis, S., Simpson, D., Friedrich, R., Jonson, J., Unger, S., and Obermeier, A.: Road traffic emissions – predictions of future contribu-
tions to regional ozone levels in Europe, Atmospheric Environment, 34, 4701–4710, https://doi.org/http://dx.doi.org/10.1016/S1352-
2310(00)00202-8, http://www.sciencedirect.com/science/article/pii/S1352231000002028, 2000.

Rieger, V. S., Mertens, M., and Grewe, V.: An advanced method of contributing emissions to short-lived chemical species (OH and HO_2):
the TAGGING 1.1 submodel
based on the Modular Earth Submodel System (MESSy 2.53), Geoscientific Model Development, 11, 2049–2066,
https://doi.org/10.5194/gmd-11-2049-2018, https://www.geosci-model-dev.net/11/2049/2018/, 2018.

Rockel, B., Will, A., and Hense, A.: The Regional Climate Model COSMO-CLM (CCLM), Meteorol. Z., 17, 347–348, 2008.

Roeckner, E., Bäuml, G., Bonaventura, L., Brokopf, R., Esch, M., Giorgetta, M., Hagemann, S., Kirchner, I., Kornblueh, L.,
Manzini, E., Rhodin, A., Schlese, U., Schulzweida, U., and Tompkins, A.: The atmospheric general circulation model ECHAM5.
PART I: Model description, MPI-Report 349, Max Planck Institut für Meteorologie in Hamburg, Deutschland, available at:
https://www.mpimet.mpg.de/fileadmin/publikationen/Reports/max_scirep_349.pdf (last access: 18 October 2015), 2003.

Roeckner, E., Brokopf, R., Esch, M., Giorgetta, M., Hagemann, S., Kornblueh, L., Manzini, E., Schlese, U., and Schulzweida, U.: Sen-
sitivity of Simulated Climate to Horizontal and Vertical Resolution in the ECHAM5 Atmosphere Model, J. Climate, 19, 3771–3791,
https://doi.org/10.1175/jcli3824.1, http://dx.doi.org/10.1175/jcli3824.1, 2006.

Sander, R., Baumgaertner, A., Gromov, S., Harder, H., Jöckel, P., Kerkweg, A., Kubistin, D., Regelin, E., Riede, H., Sandu, A., Tarabor-
relli, D., Tost, H., and Xie, Z.-Q.: The atmospheric chemistry box model CAABA/MECCA-3.0, Geosci. Model Dev., 4, 373–380,
https://doi.org/10.5194/gmd-4-373-2011, http://www.geosci-model-dev.net/4/373/2011/, 2011.

Sartelet, K. N., Couvidat, F., Seigneur, C., and Roustan, Y.: Impact of biogenic emissions on air quality over Europe and North America,
Atmospheric Environment, 53, 131 – 141, https://doi.org/https://doi.org/10.1016/j.atmosenv.2011.10.046, http://www.sciencedirect.com/

science/article/pii/S1352231011011253, aQMEII: An International Initiative for the Evaluation of Regional-Scale Air Quality Models - Phase 1, 2012.

Simpson, D.: Biogenic emissions in Europe: 2. Implications for ozone control strategies, Journal of Geophysical Research: Atmospheres, 100, 22 891–22 906, https://doi.org/10.1029/95JD01878, https://agupubs.onlinelibrary.wiley.com/doi/abs/10.1029/95JD01878, 1995.

5   Solmon, F., Sarrat, C., Serça, D., Tulet, P., and Rosset, R.: Isoprene and monoterpenes biogenic emissions in France: Modeling and impact during a regional pollution episode, Atmospheric Environment, 38, 3853–3865, https://doi.org/10.1016/j.atmosenv.2004.03.054, https://www.scopus.com/inward/record.uri?eid=2-s2.0-2942739177&doi=10.1016%2fj.atmosenv.2004.03.054&partnerID=40&md5= 86b1a697e6d7d1b1ed4f7d550b54bbcd, cited By 41, 2004.

Stevenson, D. S., Dentener, F. J., Schultz, M. G., Ellingsen, K., van Noije, T. P. C., Wild, O., Zeng, G., Amann, M., Atherton, C. S., Bell, N.,
10   Bergmann, D. J., Bey, I., Butler, T., Cofala, J., Collins, W. J., Derwent, R. G., Doherty, R. M., Drevet, J., Eskes, H. J., Fiore, A. M., Gauss, M., Hauglustaine, D. A., Horowitz, L. W., Isaksen, I. S. A., Krol, M. C., Lamarque, J.-F., Lawrence, M. G., Montanaro, V., Müller, J.-F., Pitari, G., Prather, M. J., Pyle, J. A., Rast, S., Rodriguez, J. M., Sanderson, M. G., Savage, N. H., Shindell, D. T., Strahan, S. E., Sudo, K., and Szopa, S.: Multimodel ensemble simulations of present-day and near-future tropospheric ozone, J. Geophys. Res. Atmos., 111, https://doi.org/10.1029/2005JD006338, http://dx.doi.org/10.1029/2005JD006338, 2006.

15   Tagaris, E., Sotiropoulou, R., Gounaris, N., Andronopoulos, S., and Vlachogiannis, D.: Impact of biogenic emissions on ozone and fine particles over Europe: Comparing effects of temperature increase and a potential anthropogenic NOx emissions abatement strategy, Atmospheric Environment, 98, 214 – 223, https://doi.org/https://doi.org/10.1016/j.atmosenv.2014.08.056, http://www.sciencedirect.com/science/article/pii/S135223101400658X, 2014.

Tagaris, E., Sotiropoulou, R. E. P., Gounaris, N., Andronopoulos, S., and Vlachogiannis, D.: Effect of the Standard Nomenclature for Air
20   Pollution (SNAP) Categories on Air Quality over Europe, Atmosphere, 6, 1119, https://doi.org/10.3390/atmos6081119, http://www.mdpi.com/2073-4433/6/8/1119, 2015.

Tanaka, K., Lund, M. T., Aamaas, B., and Berntsen, T.: Climate effects of non-compliant Volkswagen diesel cars, Environmental Research Letters, 13, 044 020, http://stacks.iop.org/1748-9326/13/i=4/a=044020, 2018.

Teixeira, E., Fischer, G., van Velthuizen, H., van Dingenen, R., Dentener, F., Mills, G., Walter, C., and Ewert, F.: Limited po-
25   tential of crop management for mitigating surface ozone impacts on global food supply, Atmos. Environ., 45, 2569 – 2576, https://doi.org/http://dx.doi.org/10.1016/j.atmosenv.2011.02.002, http://www.sciencedirect.com/science/article/pii/S135223101100118X, 2011.

Terrenoire, E., Bessagnet, B., Rouïl, L., Tognet, F., Pirovano, G., Létinois, L., Beauchamp, M., Colette, A., Thunis, P., Amann, M., and Menut, L.: High-resolution air quality simulation over Europe with the chemistry transport model CHIMERE, Geoscientific Model Development,
30   8, 21–42, https://doi.org/10.5194/gmd-8-21-2015, https://www.geosci-model-dev.net/8/21/2015/, 2015.

Tie, X., Brasseur, G., and Ying, Z.: Impact of model resolution on chemical ozone formation in Mexico City: application of the WRF-Chem model, Atmos. Chem. Phys., 10, 8983–8995, https://doi.org/10.5194/acp-10-8983-2010, http://www.atmos-chem-phys.net/10/8983/2010/, 2010.

Tost, H., Jöckel, P., Kerkweg, A., Sander, R., and Lelieveld, J.: Technical note: A new comprehensive SCAVenging submodel for global atmo-
35   spheric chemistry modelling, Atmos. Chem. Phys., 6, 565–574, https://doi.org/10.5194/acp-6-565-2006, http://www.atmos-chem-phys.net/6/565/2006/, 2006a.

Tost, H., Jöckel, P., and Lelieveld, J.: Influence of different convection parameterisations in a GCM, Atmos. Chem. Phys., 6, 5475–5493, https://doi.org/10.5194/acp-6-5475-2006, http://www.atmos-chem-phys.net/6/5475/2006/, 2006b.

Tost, H., Jöckel, P., and Lelieveld, J.: Lightning and convection parameterisations – uncertainties in global modelling, Atmos. Chem. Phys., 7, 4553–4568, https://doi.org/10.5194/acp-7-4553-2007, http://www.atmos-chem-phys.net/7/4553/2007/, 2007.

Tost, H., Lawrence, M. G., Brühl, C., Jöckel, P., The GABRIEL Team, and The SCOUT-O3-DARWIN/ACTIVE Team: Uncertainties in atmospheric chemistry modelling due to convection parameterisations and subsequent scavenging, Atmos. Chem. Phys., 10, 1931–1951, https://doi.org/10.5194/acp-10-1931-2010, http://www.atmos-chem-phys.net/10/1931/2010/, 2010.

Valverde, V., Pay, M. T., and Baldasano, J. M.: Ozone attributed to Madrid and Barcelona on-road transport emissions: Characterization of plume dynamics over the Iberian Peninsula, Science of The Total Environment, 543, Part A, 670 – 682, https://doi.org/http://dx.doi.org/10.1016/j.scitotenv.2015.11.070, http://www.sciencedirect.com/science/article/pii/S0048969715310500, 2016.

Vinken, G. C. M., Boersma, K. F., Maasakkers, J. D., Adon, M., and Martin, R. V.: Worldwide biogenic soil NO_x emissions inferred from OMI NO_2 observations, Atmos. Chem. Phys., 14, 10 363–10 381, https://doi.org/10.5194/acp-14-10363-2014, http://www.atmos-chem-phys.net/14/10363/2014/, 2014a.

Vinken, G. C. M., Boersma, K. F., van Donkelaar, A., and Zhang, L.: Constraints on ship NO_x emissions in Europe using GEOS-Chem and OMI satellite NO_2 observations, Atmospheric Chemistry and Physics, 14, 1353–1369, https://doi.org/10.5194/acp-14-1353-2014, https://www.atmos-chem-phys.net/14/1353/2014/, 2014b.

Wang, Z. S., Chien, C.-J., and Tonnesen, G. S.: Development of a tagged species source apportionment algorithm to characterize three-dimensional transport and transformation of precursors and secondary pollutants, Journal of Geophysical Research: Atmospheres, 114, n/a–n/a, https://doi.org/10.1029/2008JD010846, http://dx.doi.org/10.1029/2008JD010846, d21206, 2009.

Wild, O.: Modelling the global tropospheric ozone budget: exploring the variability in current models, Atmospheric Chemistry and Physics, 7, 2643–2660, https://doi.org/10.5194/acp-7-2643-2007, http://www.atmos-chem-phys.net/7/2643/2007/, 2007.

Wild, O. and Prather, M. J.: Global tropospheric ozone modeling: Quantifying errors due to grid resolution, J. Geophys. Res. Atmos., 111, n/a–n/a, https://doi.org/10.1029/2005JD006605, http://dx.doi.org/10.1029/2005JD006605, d11305, 2006.

World Health Organization: Health aspect of air pollution with particulate matter, ozone and nitrogen dioxide, World Health Organization, Bonn, 2003.

Yan, Y., Pozzer, A., Ojha, N., Lin, J., and Lelieveld, J.: Analysis of European ozone trends in the period 1995–2014, Atmospheric Chemistry and Physics, 18, 5589–5605, https://doi.org/10.5194/acp-18-5589-2018, https://www.atmos-chem-phys.net/18/5589/2018/, 2018.

Yienger, J. J. and Levy, H.: Empirical model of global soil-biogenic NOx emissions, Journal of Geophysical Research: Atmospheres, 100, 11 447–11 464, https://doi.org/10.1029/95JD00370, http://dx.doi.org/10.1029/95JD00370, 1995.

Table 1. Overview of the most important submodels applied in EMAC and COSMO/MESSy, respectively. Both COSMO/MESSy instances use the same set of submodels. MMD* comprises the MMD2WAY submodel and the MMD library.

Submodel	EMAC	COSMO	short description	references
AEROPT	x		calculation of aerosol optical properties	Dietmüller et al. (2016)
AIRSEA	x	x	exchange of tracers between air and sea	Pozzer et al. (2006)
CH4	x		methane oxidation and feedback to hydrological cycle	
CLOUD	x		cloud parametrisation	Roeckner et al. (2006), Jöckel et al. (2006)
CLOUDOPT	x		cloud optical properties	Dietmüller et al. (2016)
CONVECT	x		convection parametrisation	Tost et al. (2006b)
CVTRANS	x	x	convective tracer transport	Tost et al. (2010)
DDEP	x	x	dry deposition of aerosols and gas phase tracers	Kerkweg et al. (2006a)
EC2COSMO	x		additional ECHAM5 fields for COSMO coupling	Kerkweg and Jöckel (2012b)
GWAVE	x		parametrisation of non-orographic gravity waves	Roeckner et al. (2003)
JVAL	x	x	calculation of photolysis rates	Landgraf and Crutzen (1998), Jöckel et al. (2006)
LNOX	x		NO_x-production by lighting	Tost et al. (2007), Jöckel et al. (2010)
MECCA	x	x	tropospheric and stratospheric gas-phase chemistry	Sander et al. (2011), Jöckel et al. (2010)
MMD*	x	x	coupling of EMAC and COSMO/MESSy (i.e. library and submodel)	Kerkweg and Jöckel (2012b); Kerkweg et al. (2018)
MSBM	x	x	multiphase chemistry of the stratosphere	Jöckel et al. (2010)
OFFEMIS	x	x	prescribed emissions of trace gases and aerosols	Kerkweg et al. (2006b)
ONEMIS	x	x	on-line calculated emissions of trace gases and aerosols	Kerkweg et al. (2006b)
ORBIT	x	x	Earth orbit calculations	Dietmüller et al. (2016)
QBO	x		Newtonian relaxation of the quasi-biennial oscillation (QBO)	Giorgetta and Bengtsson (1999), Jöckel et al. (2006)
RAD	x		radiative transfer calculations	Dietmüller et al. (2016)
SCAV	x	x	wet deposition and scavenging of trace gases and aerosols	Tost et al. (2006a)
SEDI	x	x	sedimentation of aerosols	Kerkweg et al. (2006a)
SORBIT	x	x	sampling along sun synchronous satellite orbits	Jöckel et al. (2010)
SURFACE	x		surface properties	Jöckel et al. (2016)
TAGGING	x	x	source apportionment using a tagging method	Grewe et al. (2017)
TNUDGE	x	x	Newtonian relaxation of tracers	Kerkweg et al. (2006b)
TROPOP	x	x	diagnostic calculation of tropopause height and additional diagnostics	Jöckel et al. (2006)

Table 2. Definition of the chemical families used in the tagging method which diagnoses the source attribution. More details on the species contained in the families are given in the Supplement of Grewe et al. (2017).

Tagged species	Description
O_3	Ozone as family of odd oxygen
PAN	PAN
CO	CO
NOy	all chemically active nitrogen compounds without PAN in the chemical mechanisms (15)
NMHC	all NMHCs in the chemical mechanisms (42)
OH	OH tagged in a steady state approach (see Rieger et al., 2018)
HO_2	HO_2 tagged in a steady state approach

Table 3. Description of the different tagging categories applied in this study following Grewe et al. (2017). Please note that some tagging categories summarise different emission sectors (see description). The last row shows the nomenclature of the tagged tracers exemplary for ozone.

tagging category	description	notation for tagged ozone
land transport	emissions of road traffic, inland navigation, railways (IPCC codes 1A3b_c_e)	O_3^{tra}
anthropogenic non-traffic	sectors energy, solvents, waste, industries, residential, agriculture	O_3^{ind}
ship	emissions from ships (IPCC code 1A3d)	O_3^{shp}
aviation	emissions from aircraft	O_3^{air}
lightning	lightning NO_x emissions	O_3^{lig}
biogenic	on-line calculated isoprene and soil-NO_x emissions, off-line emissions from biogenic sources and agricultural waste burning (IPCC code 4F)	O_3^{soi}
biomass burning	biomass burning emissions	O_3^{bio}
CH_4	degradation of CH_4	O_3^{CH4}
N_2O	degradation of N_2O	O_3^{N2O}
stratosphere	downward transport from the stratosphere	O_3^{str}

Table 4. Average (2008 to 2010) annual total emissions for the CM50 domain of different anthropogenic emission sectors for NO_x (in $Tg(NO) \, a^{-1}$), CO ($Tg(CO) \, a^{-1}$), VOC ($Tg(C) \, a^{-1}$) and the NO_x to VOC ratio (NO_x/VOC)).

emission sector	REF				EVEU			
	NO_x	CO	VOC	NO_x/VOC	NO_x	CO	VOC	NO_x/VOC
land transport	5.2	29	3.1	1.7	5.4	24	3.4	1.6
anthropogenic non traffic	7.3	28	14	0.52	5.1	30	6.5	0.78
shipping	2.4	0.25	0.36	6.5	1.8	0.30	0.096	19
aviation	0.60	-	-	-	0.55	-	-	-

Table 5. Average (2008–2010) annual total emissions for the CM50 domain of NO_x (in $Tg(NO)\,a^{-1}$), CO ($Tg(CO)\,a^{-1}$), VOC ($Tg(C)\,a^{-1}$) and the NO_x to VOC ratio (NO_x/VOC). Given are the total emissions of the emission sectors which are identical in *REF* and *EVEU*.

emission sector	NO_x	CO	VOC	NO_x/VOC
biogenic	1.2	4.8	22	0.056
biomass burning	0.26	9.0	0.377	0.73
agricultural waste burning	0.081	2.845	0.0981	0.83
lightning	0.76	-	-	-

Table 6. Contribution of different emission source area averaged over Europe (defined as rectangular box $10°$ W to $38°$ E and $30°$ N to $70°$ E) for JJA 2008–2010 at three different altitudes (in %). The values are mean values of the *REF* and *EVEU* simulation, the range indicates the standard deviation between the results of *REF* and *EVEU*.

	ground	600 hPa	200 hPa
stratosphere	7.4 ± 0.1	13.7 ± 0.1	52.0 ± 0.1
CH_4	14.3 ± 0.1	14.7 ± 0.1	8.3 ± 0.1
lightning	8.8 ± 0.2	15.0 ± 0.5	9.0 ± 0.1
aviation	3.7 ± 0.1	5.2 ± 0.1	2.0 ± 0.1
biomass burning	6.1 ± 0.1	4.8 ± 0.1	2.2 ± 0.1
biogenic	18.8 ± 0.3	15.7 ± 0.1	7.5 ± 0.1
shipping	9.2 ± 0.6	4.7 ± 0.1	1.5 ± 0.1
anth. non-traffic	16.4 ± 0.8	13.0 ± 0.2	6.1 ± 0.1
land transport	11.6 ± 0.4	8.3 ± 0.1	3.3 ± 0.1
N2O	3.6 ± 0.1	5.1 ± 0.0	8.3 ± 0.1

Table 7. Diagnosed net ozone production (P_{O3}) of the ten considered categories (in $Tg\ a^{-1}$) as simulated by CM50. The production rates are integrated over the CM50 domain and up to 850/200 hPa, respectively. The values are averaged for 2008–2010, the ranges indicate one standard deviation with respect to time based on the annual averages from the years 2008–2010.

	P_{O3} integrated up to 850 hpa ($Tg\ a^{-1}$)		P_{O3} integrated up to 200 hpa ($Tg\ a^{-1}$)	
	REF	EVEU	REF	EVEU
land transport	13.2 ± 0.2	13.3 ± 0.3	22.8 ± 0.6	23.4 ± 0.5
anthropogenic non-traffic	22.2 ± 0.5	15.1 ± 0.3	37.8 ± 1.1	26 ± 0.5
shipping	6.7 ± 0.1	5.6 ± 0.1	10.6 ± 0.1	8.8 ± 0.1
aviation	0.3 ± 0.1	0.1 ± 0.1	8.1 ± 0.1	7.9 ± 0.1
biogenic	15.9 ± 0.6	15.3 ± 0.5	28.8 ± 0.7	28.2 ± 0.7
lightning	-0.9 ± 0.1	-1.0 ± 0.1	6.9 ± 0.3	7.0 ± 0.3
biomass burning	2.1 ± 0.2	1.8 ± 0.1	3.8 ± 0.3	3.5 ± 0.3
CH_4 degradation	4.5 ± 0.1	3.6 ± 0.1	12.5 ± 0.4	11.5 ± 0.4
N_2O	-0.2 ± 0.1	-0.3 ± 0.1	1.8 ± 0.1	1.7 ± 0.1
stratosphere	-1.9 ± 0.1	-1.7 ± 0.6	-10.9 ± 0.7	-11 ± 0.7
total	61.8 ± 0.3	51.9 ± 1.0	122.3 ± 2.0	107.4 ± 1.8